HIGH RESOLUTION MOLECULAR CHARACTERIZATION OF PHOTOCHEMICAL AND MICROBIAL TRANSFORMATION OF DISSOLVED ORGANIC MATTER IN TEMPERATE STREAMS OF DIFFERENT WATERSHED LAND USE

by

XIAPING LI

YUEHAN LU, COMMITTEE CHAIR
CHUNMIAO ZHENG, CO-CHAIR
NATASHA T. DIMOVA
ROBERT FINDLAY

A THESIS

Submitted in partial fulfillment of the requirements
for the degree of Master of Science in the
Department of Geological Sciences
in the Graduate School of
The University of Alabama

TUSCALOOSA, ALABAMA

2014

Copyright Xiaping Li 2014
ALL RIGHTS RESERVED

ABSTRACT

The objective of the present study was to provide better understanding of the effects of watershed land use on molecular composition of streamwater DOM and molecular transformations associated with photochemical and microbial processing of DOM. We compared DOM from headwater streams draining forest-dominated watersheds (FW) and pasture-dominated watersheds (PW) in the lower Chesapeake Bay region (Virginia, USA). Electrospray Ionization Fourier Transform Ion Cyclotron Resonance Mass Spectrometry analysis was conducted on streamwater DOM prior to and after laboratory incubations: 1) bacteria-only incubations; 2) light-only incubations; and 3) combined light+bacterial incubations. Results showed that DOM in FW streams and PW streams differed in molecular characteristics—the former was characterized by greater structural complexity and aromaticity, higher proportions of condensed aromatic molecules and black carbon-like components, while the latter was higher in the proportions of lipid-like components, protein-like components and aliphatic compounds. Relative to DOM from FW streams, DOM from PW streams was more reactive to bacterial transformation. Protein-like components, lipid-like components and unsaturated hydrocarbon-like components are primarily responsible for the changes associated with bacterial transformation of DOM. However, similar behavior was also observed for DOM in FW streams and PW streams under the influence of bacterial and photochemical processes. Bacterial transformation reduced the proportions of lipid-like components but increased the proportions of lignin-like components and carboxyl-rich alicyclic molecule-like components, indicating that lipid-like components was a bioreactive class while lignin-like components and carboxyl-rich

alicyclic were resistant to bacterial processing. Photochemical processes, alone or combined with microbial alterations, increased the proportions of protein-like components, which may be due to the light stimulation of autochthonous production of protein-like components, and increased the relative abundance of carboxyl-rich alicyclic molecule-like components, which indicates the refractory nature of these molecules. Photochemical processes also significantly reduced the amount of dissolved black carbon-like components, which suggests dissolved black carbon was a photoreactive class, countering the conventional view that black carbon was an inter group in carbon cycle. Collectively, these findings suggest that human land use in upstream watersheds may lead to alterations to the molecular composition of streamwater DOM as well as to its behavior to photochemical and microbial processing.

DEDICATION

This thesis is dedicated to my grandparents, Mr. and Mrs. Li.

LIST OF ABBREVIATIONS AND SYMBOLS

AI	Aromaticity index
C	Carbon
DBE	Double bond equivalent
DOC	Dissolved organic carbon
DOM	Dissolved organic matter
ESI	Atmospheric pressure electrospray ionization
FTICR-MS	Fourier Transform Ion Cyclotron Resonance Mass Spectrometry
FW	Forest-dominated watershed
H	Hydrogen
M_n	Number-average molecular weight
M_w	Weight-average molecular weight
MW	Molecular weight
N	Nitrogen
P	Phosphorous
PW	Pasture-dominated watershed
S	Sulfur
T_0	Time point, prior to incubations
T_{15}	Time point, after incubations

ACKNOWLEDGMENTS

I would like to express my deep appreciation and gratitude to my advisors, Dr. Yuehan Lu and Dr. Chunmiao Zheng, for the special opportunity to work on this project and the patient guidance and mentorship they provided to me. I would like to thank my committee members, Dr. Natasha Dimova and Dr. Robert Findlay for the guidance and thoughtful suggestions. I would also like to thank the faculty, staff, and students of the University of Alabama for friendly suggestions.

I want to express my appreciation to Rajaa Mesfioui and other members of Dr. Patrick Hatcher's Group at the Department of Chemistry and Biochemistry, Old Dominion University for generous and patient guidance on sample analysis by using ESI-FTICR-MS and data processing. I would also like to thank Dr. James Bauer, Dr. Elizabeth Canuel, Dr. R. M. Chambers for thought-provoking suggestions.

I appreciate the Johnson Fund and the Hook's Fund of Department of Geological Sciences at the University of Alabama, Graduate School Research and Travel Support Fund of the University of Alabama, College of Arts and Sciences Travel Funding of the University of Alabama, Mellon Foundation of the College of William and Mary. Thank you for support in financial aid.

I would like to thank Dr. Maosheng Zhang. He was always encouraging me to overcome challenges during studying abroad.

Finally, I would like to thank my loving family for support in financial aid and encouragements. They were always there cheering me up and stood by me.

CONTENTS

LIST OF TABLES

LIST OF FIGURES

CHAPTER 1

INTRODUCTION

Dissolved organic matter (DOM) in aquatic environments represents an important component of the global C cycle (e.g., ~90% of organic carbon in the oceans is DOM) (Mopper et al., 2007) and serves as the basal energy and food source to aquatic food webs (Cole and Caraco, 2001; Gennings et al., 2001; Aufdenkampe et al., 2011). In freshwaters, an important fraction of DOM is derived from surrounding watersheds and this fraction is referred to as "allochthonous DOM" (as opposed to "autochthonous DOM", referring to DOM derived from organisms living in water, particularly algae and microbes; Figure 1) (Cole and Caraco, 2001). Following its export from watersheds, allochthonous DOM undergoes photochemical and microbial transformation (Obernosterer and Benner, 2004), in which DOM is either remineralized into inorganic constituents (e.g., CO_2, nitrate) or altered to smaller molecules that are generally more bioavailable (Benner, 2003; Kirchman, 2003). Allochthonous DOM therefore plays a pivotal role in determining CO_2 fluxes among terrestrial, aquatic and atmospheric reservoirs, as well as energy and substrate transfer in aquatic food webs (Cole and Caraco, 2001; Gennings et al., 2001; Aufdenkampe et al., 2011).

Human land use, by changing terrestrial landscapes and soil environments globally (Foley et al., 2005), has altered the properties of allochthonous DOM and its photochemical and microbial processing. A few recent studies have shown that human land use may alter the sources, ages, molecular weights, structure and reactivity of DOM in stream and rivers (Wilson and Xenopoulos, 2009; Williams et al., 2010; Stanley et al., 2012; Lu et al., 2013). For instance, Williams et al. (2010) showed that *in situ* microbial activity may be higher in streams within watersheds modified by human land use than those with less anthropogenic modification, suggesting land

use may stimulate microbial food webs by providing greater amounts of molecules labile for heterotrophic bacterial utilization. Lu et al. (2013) observed that DOM derived from forested watersheds decomposed faster under light than DOM from agricultural and urban watersheds. This observation suggests that human land use may decrease DOM photoreactivity, which potentially contributes to the decadal increases in the concentrations of DOC from North American and Europe freshwaters (Clark et al., 2010; Clair et al., 2011) and the formation of coastal dead zones (Bianchi et al., 2010).

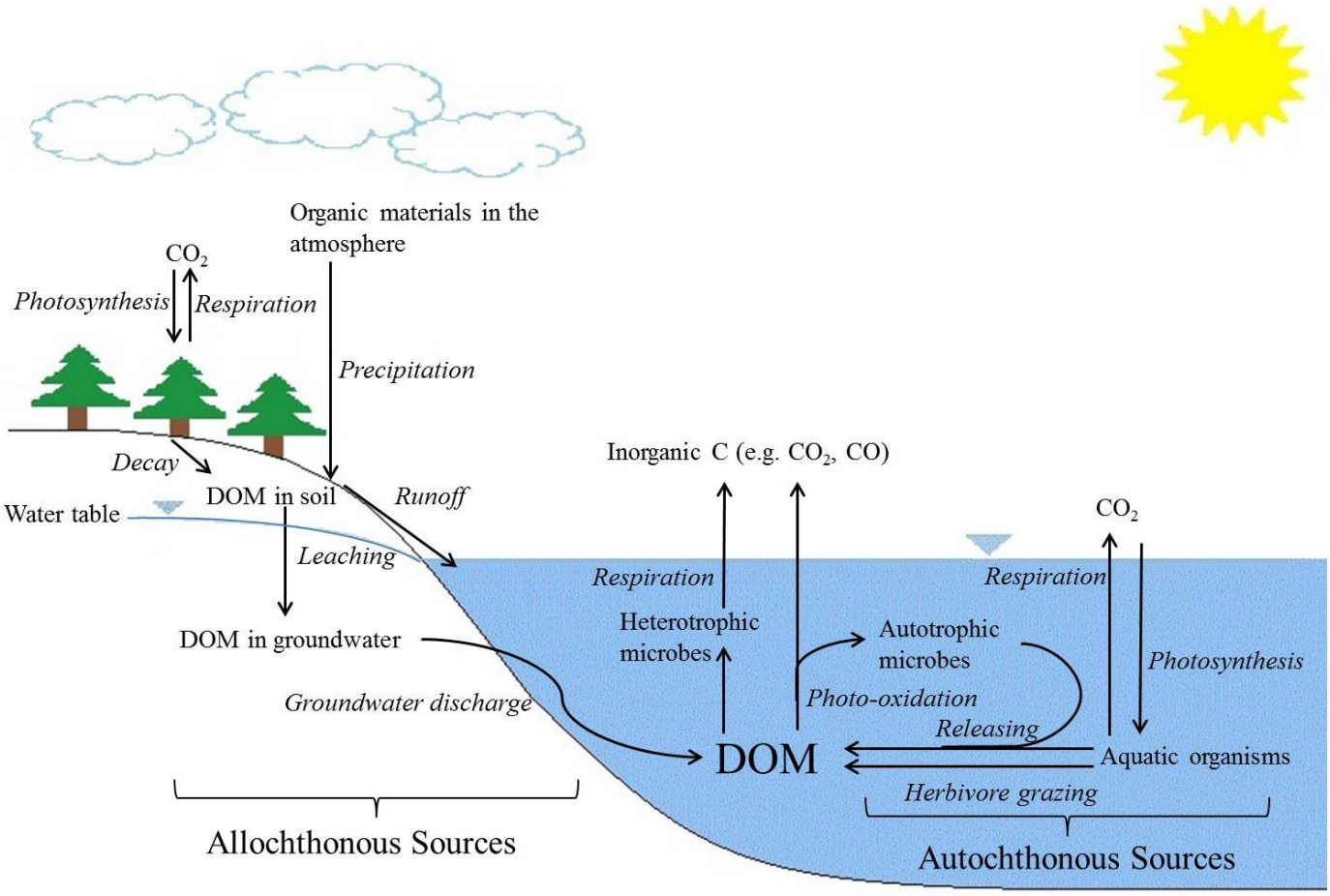

Figure 1. Schematic illustration of the sources, transportation and transformation of DOM in terrestrial and aquatic environments.

While human land use may lead to substantial changes in freshwater DOM that have important implications for a variety of key environmental and ecosystem processes, these changes have not been well understood at the molecular level. Previous studies mostly used fluorescence and isotopic techniques to characterize the bulk DOM pool (e.g., Wilson and Xenopoulos, 2009; Williams et al., 2010; Lu et al., 2013), yielding limited information about how land use altered DOM at the molecular level and hindering an unambiguous identification of the mechanisms responsible for the observed DOM alterations. For example, Lu et al. (2013) hypothesized that the variability of DOC bioreactivity from streams draining different types of land use may be associated with the diagenetic status of DOM, while no conclusive evidence was provided because the isotopic and fluorescence analyses have limited power in distinguishing between bioreactive *vs.* biorefractory DOM molecules. Likewise, several researchers observed that microbial reactivity in streams may be enhanced by agricultural land use (Wilson and Xenopoulos, 2009; Williams et al., 2010) but it remains uncertain whether this enhancement is driven by the changes in the molecular composition of DOM or other relevant processes (e.g., nutrient enrichment). Therefore, detailed information about molecular constituents of DOM is crucial to form better understanding of the mechanisms underlying the widespread changes in freshwater DOM due to human land use.

The scarcity of molecular DOM data is largely due to the inherent complexity of DOM composition, characterized by a mixture of Low-Molecular-Weight (LMW) substances and High-Molecular-Weight (HMW) biomolecules that cannot be separated and identified by conventional, low-resolution instrumental approaches (Mopper et al., 2007). Fourier Transform Ion Cyclotron Resonance Mass Spectrometry (FTICR-MS), offering ultrahigh resolution for identification of ionized organic compounds, has been demonstrated as a powerful instrumental

approach in characterizing DOM at the molecular level (Nebbioso and Piccolo, 2013). A great number of individual fulvic acid molecules were firstly determined by employing FTICR-MS (Stenson et al., 2003). Atmospheric pressure electrospray ionization (ESI) technique can ionize water-soluble, hydrophilic molecules with no or negligible fragmentation (Kujawinski and Behn, 2006; Mopper et al., 2007). Combining ESI with FTICR-MS, Sleighter and Hatcher (2008) successfully resolved thousands of DOM components along a river-fluvial-ocean transect in lower Chesapeake Bay.

In the present study, we used ESI-FTICR-MS to analyze DOM from temperate headwater streams draining watersheds dominated by two different types of land use (Forest and Pasture). The objective was to characterize how DOM exported from watersheds of varying land use differs in its composition and its photochemical and microbial transformations at the molecular level. We sampled a regional group of streams influenced by similar geological and meteorological variables during base flow periods in order to minimize DOM variability associated with geological, climatic and hydrological parameters (Bertilsson and Jones, 2003; Mattsson et al., 2005; Stanley et al., 2012) and thereby highlight the effects of land use. Three different types of laboratory incubations, i.e., light-only incubation, bacterial-only incubation, combined light + bacterial incubation, were conducted for characterizing DOM molecular transformations under the influence of photochemical and microbial processes.

CHAPTER 2

METHODS

2.1 Sample Collection, Filtration and Incubation

Our study site includes four headwater streams located within the watershed of Mattaponi River, a tributary of the York River discharging to the Chesapeake Bay, Virginia, USA (Figure 2). The streams were around 1–6 km apart. Two of the streams (F1, F2) were situated within watersheds dominated by oak-pine forest (hereinafter referred to as "FW streams"). The other two streams (P1, P2) drained pasture-dominated watersheds (hereinafter referred to as "PW streams"), where pastures were annually rotated between warm-season grasses (May–October) and cool-season grasses (November–April).

All streams were sampled during base flow conditions in November, 2009. A suite of *in situ* parameters were measured (Table 1). Stream water samples were collected in 20 l polycarbonate carboys using a Masterflex® E/S™ portable sampler (Cole-117 Parmer) equipped with acid-cleaned silicone tubing. After collection, samples were stored on ice in the dark for up to 6 hours until being filtrated in the lab. Living and non-living particulate materials were removed by filtering water through pre-baked GF/F glass fiber filters (nominal pore sizeof 0.7 μm) (McCallister et al., 2004). In order to remove bacteria, a portion of the 0.7 μm filtrate was then subsequently filtered through a 0.2 μm capsule filter (Whatman polycap; pre-cleaned with 10% HCl and distilled water). Bacterial removal was confirmed by direct counting of bacteria using Fluorescence Microscopy method (Parsons et al., 1994). Laboratory incubations were started immediately after filtration process. All incubations lasted 15 days, including three

treatment types: 1) dark, bacteria-only treatment, i.e., 0.7 µm filtrate in the dark, 2) bacteria-free, light-only treatment, i.e., 0.2 µm filtrate incubated under light, and 3) combined light+bacteria treatment, i.e., 0.7 µm filtrate under light. The incubation temperature for all experiments was controlled at 22±2˚C.

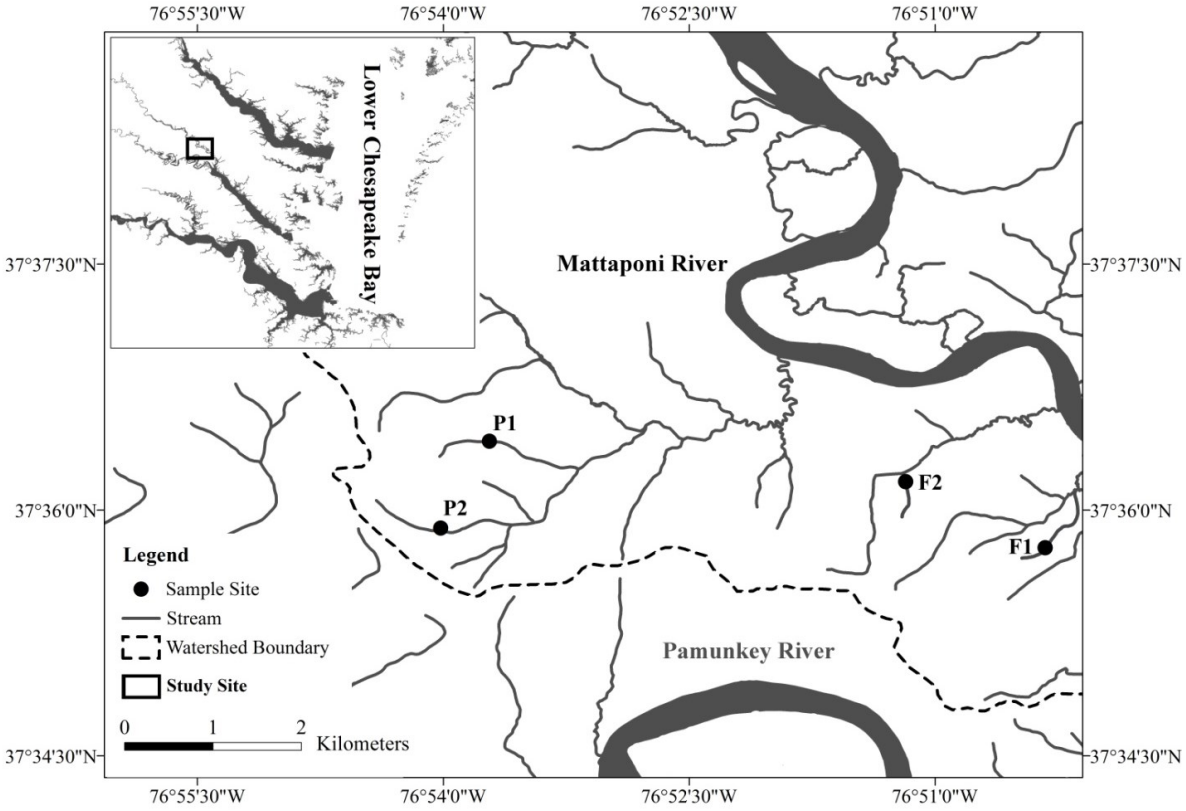

Figure 2. Study Sites.

Light incubations were performed in 500 ml quartz flasks on a rotating light table. The detailed description of the light source can be found in Lu et al. (2013). Briefly, the light source has spectral light similar to that of natural sunlight from the UV wavelengths between 295 and 365 nm (Dalzell et al., 2009; Spencer et al., 2009). In the 15 day-light incubations, the samples were exposed to light for 24 h per day, receiving UV exposure equivalent to 10 days of 12 h daylight at the sampling sites. Dark incubations were conducted in 1000 ml amber borosilicate glass bottles, which were placed in dark bags to further prevent light penetration.

Table 1. Environmental parameters, watershed land use and DOC concentrations of the sampling streams (Data source: Lu et al, 2013).

Sampling site	Water Temperature (℃)	Specific Conductivity (µS)	pH	Dissolved Oxygen (mg/L)	Watershed Land Use Composition	DOC Concentration (µM)	Chlorophyll-a (µg/L)	Nitrate (mg/L)	Ammonium (mg/L)
F1	12.6	158.9	5	3.0	100% forest	539	0.01	b.d.	b.d.
F2	12.6	56.9	5	7.8	100% forest	562	0.05	b.d.	b.d.
P1	12.6	210.4	6~7	7.9	70% pasture, 30% forest	675	0.14	2.29	2.49
P2	16.5	73.4	5	5.8	61% pasture, 39% forest	206	0.48	b.d.	b.d.

b.d.=below detection

2.2 ESI-FTICR-MS

Samples at the beginning and end of the incubation (T_0 and T_{15}, respectively) were analyzed using ESI-FTICR-MS at the College of Science Major Instrumentation Cluster (COSMIC) Lab, Old Dominion University (Virginia, USA). We used C_{18} extraction method to concentrate DOM, which selectively retain non-polar low-molecular-weight DOM (LMW-DOM; <700Da) (Kim et al., 2003a). Solid phase C_{18} extraction disks (3M, Empore™, 47-mm) were activated by LC-MS grade water and methanol before use. Sample waters were acidified to pH = 2 before passing through C_{18} disks under vacuum. Water and methanol (LC-MS grade) then were used sequentially to elute off materials retained on C_{18} disks. The elutes were collected, diluted with LC-MS grade water to obtain the ratio of 50:50 (v/v) methanol:water for each sample, and then added with ammonium hydroxide to bring up the pH value to 8 for increasing ionization efficiency (Sleighter and Hatcher, 2008).

All samples were continuously infused into an Apollo II ESI ion source of a Bruker Daltonics 12 Tesla Apex Qe FTICR-MS, using a syringe pump providing an infusion rate of 120μL/h. A solution of 0.1% ammonium hydroxide in 50:50 (v/v) methanol:water was analyzed between each sample, serving as a blank for sample cross-contamination check (Stubbins et al., 2010). The samples and blanks were analyzed in negative ion mode and electrospray voltages were made effective for each sample. Ions accumulated in a hexapole for 1.0 s before traveling to the ion cyclotron resonance cell. 300 or 350 transients were added and collected with a 4 MWord time domain, yielding a total run time of 30 or 35 minutes, respectively. The summed free induction decay signal was zero-filled once and Sine-Bell apodized prior to fast Fourier transformation and magnitude calculation using the Bruker Daltonics Data Analysis software.

2.3 Calibration and Molecular Formula Assignments

All masses were internally calibrated following the calibration method described in Sleighter et al. (2008), using fatty acid naturally present within our samples and other homologous peak series identified by Kendrick mass defect (KMD) analysis, which spanned the entire mass range of 200-700 m/z. Only m/z values with signal to noise ratios above 4 were considered for formula assignment formulae. A molecular formula calculator developed at National High Magnetic Field Laboratory in Tallahassee, FL (Molecular Formula Calc v.1.0 ©NHMFL, 1998) was used to generate empirical formulae. The range of the number of different atoms was set as: 1–50 for carbon, 2–100 for hydrogen, 0–30 for oxygen, 0–6 for nitrogen and 0–2 for sulfur. Data processing was previously described in detail by Sleighter and Hatcher (2007) and Stubbins et al. (2010). In brief, we first chose the chloride-free peaks with the difference between measured mass and exact mass of the empirical formulae within ±1 ppm. We then eliminated empirical formulae that did not comply with the basic bonding criteria of organic compounds as follows (Zhong et al., 2011; Mopper et al., 2007): 1) $O/C \leq 1.2$; 2) $0.35 \leq H/C \leq 2.25$; 3) $N/C \leq 0.5$; 4) $S/C \leq 0.2$; 5) nitrogen rule (i.e., odd mass weight containing even-electron N ions, while even mass weight containing odd-electron N ions); 6) Double Bond Equivalent (DBE) value is an integer ≥ 0. DBE is calculated as below:

$$DBE = (2+2*\#C-\#H+\#N+\#P)/2 \qquad \text{Eqn (1)}$$

Where *#C*, *#H*, *#N* and *#P* represent the number of carbon, hydrogen, nitrogen, and phosphorous atoms in molecules, respectively. Lastly, we applied KMD analysis to ensure assigned formulae fell into homologous series.

2.4 Statistical Analysis

Jaccard similarity coefficients were calculated to analyze the similarity of DOM molecules between different samples. Linear regression analysis was used to assess the relationship between changes in percentages of biochemical classes and jaccard similarity coefficients.

CHAPTER3

RESULTS AND DISCUSSIONS

3.1 Interpretation Proxies

3.1.1 Molecular Weight

Molecular weight (MW) may provide important information about the structure and chemical reactivity of DOM (Chin et al., 1994). In the present study, two types of MW, weight-average MW (M_w) and number-average MW (M_n) were calculated:

$$M_w = \sum_{i=1}^{n} I_i \Big/ \sum_{i=1}^{n} \frac{I_i}{M_i} \qquad \text{Eqn (2)}$$

$$M_n = \sum_{i=1}^{n} I_i * M_i \Big/ \sum_{i=1}^{n} I_i \qquad \text{Eqn (3)}$$

where *n* represents the number of molecules for each sample, M_i is the observed m/z ratio and I_i is the intensity of the corresponding peak (Dalzell et al., 2009; Kim et al., 2006). Assumptions underlying the calculation of M_w and M_n include that the ions are singly charged over the entire scan range and the abundance of each ion is proportional to the intensity of the corresponding peak (Piccolo and Spiteller, 2003). Although these two types of molecular weights have their respective limitations and thus may not represent the actual molecular weight, their ratios (M_w/M_n) yielded important information about DOM mass distribution (Dalzell et al., 2009). A greater M_w/M_n value represents a wider molecular mass distribution, i.e., peak height is more evenly distributed among different masses (Cooper, 1989).

3.1.2 Van Krevelen Analysis

Van Krevelen analysis classifies the DOM molecules into different biochemical classes based on their O/C and H/C atomic ratios (Kim et al., 2003b; Sleighter and Hatcher, 2007). The use of Van Krevelen diagram involves two assumptions: 1) all molecules have the same ionization efficiency; and 2) charged molecules do not experience ion-molecule reactions (Kim et al., 2003b).

In the present study, six biochemical classes were defined (Hockaday et al., 2009; Ohno et al., 2010): 1) lipids (H/C = 1.5-2.0, O/C = 0-0.3); 2) proteins (H/C = 1.5-2.2, O/C =0.3-0.67); 3) lignins (H/C = 0.7-1.5, O/C=0.1-0.67); 4) carbohydrates (H/C = 1.5-2.4, O/C = 0.67-1.2); 5) unsaturated hydrocarbons (H/C = 0.7-1.5, O/C= 0-0.1); and 6) condensed aromatic structures (H/C = 0.2-0.7,O/C = 0-0.67) (Figure 4).

3.1.3 Index Analysis

Several indices have been commonly used to characterize DOM compounds into different groups. The modified aromaticity index (AI) (Eqn 4) was used to identify aromatic compounds (AI > 0.5) and condensed aromatic structures (AI >0.67) (Koch and Dittmar, 2006).

$$AI=\frac{1+\#C-0.5\#O-\#S-0.5\#H}{\#C-0.5\#O-\#S-\#N-\#P} \qquad \text{Eqn (4)}$$

Aliphatic compounds were defined as molecules with DBE/C < 0.3 and H/C >1 (Perdue, 1984), while black carbon were defined as molecules with O/C ratio between 0.3 and 0.6 and H/C less than 0.8 (Kim et al., 2004). Molecules with DBE/C >0.7 or AI>0.67 were thought to contain condensed aromatic structures (Hockaday et al., 2006; Koch and Dittmar, 2006), while molecules of DBE/C between 0.3 – 0.68, DBE/O between 0.77 – 1.75 and DBE/H between 0.2–0.95 were presumably carboxyl-rich alicyclic molecule (Hertkorn et al., 2006).

3.2 Data Reproducibility

No standard measures are available to assess data reproducibility between different FT-ICRMS runs and/or uncertainties arising from formula assignment. It has been observed that FT-ICRMS data could vary with DOM extraction, instrumental parameters and performance, ionization efficiency and approaches of formula assignment (Kim, et al., 2003b; Kujawinski et al., 2004; Simjouw et al. 2005; Kujawinski and Behn, 2006; Koch et al., 2007; Mopper et al., 2007). For example, higher magnetic field strength may result in better mass resolution (Mopper et al., 2007). Koch et al. (2007) summarized the three common approaches of formula assignment: 1) a priori exclusion of elements and "best fit" based on the extrapolation , which may be unsuitable when the calculated mass is within the analytical error (i.e. 1ppm); 2) a posteriori exclusion of elements based on molecular information from the actual mass spectrum, which is suitable only for peaks with high signal to noise ratios (S/N > 20) and without N atom; and 3) a "chemical building block" method that uses functional groups (i.e. CH_2, COOH) of molecules and may not be efficient for the observed mass greater than 350 Da. Additionally, these researchers proposed a stable carbon isotope approach which was considered beneficial to prevent false identification of abundant ions. Combined with basic molecular information, functional groups and carbon isotope, we assigned each peak with only one "best fit" formula.

In the present study, the data reproducibility was evaluated by comparing P1 (0.7μm filtration) at T_0 and an abiotic control (0.2μm filtration, 15-day dark incubation) for P1 (P1*). The control sample had not been processed by photochemical or bacterial processes and theoretically should have the same components with P1 at T_0. The jaccard similarity coefficient showed that the abiotic control and P1 at T_0 shared 63.8% of DOM molecular formulae (Table 2).

The different filtration methods used to control bacteria presence may also contribute to the variability of DOM components. The 0.7 μm filtrate *vs.* 0.2 μm filtrate of the same sample (F1 at T_0) shared 65.9% of DOM molecular formulae (Table 2). Therefore, the variation associated with pre-treatment procedures (i.e., filtration and incubation) and FTICR-MS runs may together result in ~40% difference in the set of DOM formulae from a sample and the relative control sample. Similarly, Mosher et al. (2010) analyzed stream water DOM in triplicate using FT-ICR-MS and found the triplicate runs, without the involvement of incubation and different filtration methods, produced DOM formulae with jaccard similarity coefficients between 0.74 and 0.8.

Table 2. Jaccard similarity coefficient defining DOM composition similarity among FW and PW streams at T_0. P1 is 0.7 μm filtrate, while P1*is the abiotic control (0.2μm filtration, 15-day dark incubation) for the P1. F1 and F1* represent the 0.7 μm filtrate and 0.2 μm filtrate of the F1 sample, respectively.

	P1	**P1***	**P2**	**F1**	**F1***	**F2**
P1	1.000	0.638	0.494	0.506	0.473	0.532
P1*		1.000	0.464	0.471	0.468	0.475
P2			1.000	0.371	0.334	0.451
F1				1.000	0.659	0.622
F1*					1.000	0.541
F2						1.000

3.3 Comparison of FW and PW Samples at T_0

3.3.1 DOM Composition Similarity

The jaccard similarity coefficient of the two FW stream samples (F1 and F2) was 0.622 (Table 2), indicating these two samples were similar and their differences were not greater than

the amount of differences attributable to operation and instrument variability. In contrast, the jaccard similarity coefficients between the two PW streams (P1 and P2) was 0.494, indicating that the differences in DOM formulae of these two samples were "real" and cannot be explained solely by operation and instrument variability (Table 2). The jaccard similarity coefficients between P2 stream *vs.* the two forest streams were smaller than the coefficients between P1 stream *vs.* the two forest streams (Table 2). This observation is consistent with that the DOC concentration in the P2 stream was smaller than P1 and the two FW streams (Table 1). In addition, the dissimilar composition of DOM in P1 *vs.* P2 may be related to the different land use composition of the watersheds of P1 and P2 (Table1). As observed by Graeber et al. (2012), the percentage of agricultural land cover within the catchments was an important factor influencing DOM composition, as shown by the fluorescence properties of DOM from 53 headwater streams with different land use compositions in central Europe.

3.3.2 Mass Distribution

FW and PW streams showed different mass distribution within their DOM pool (Figure 3). Both samples from FW streams had highest peaks concentrated in the range of 280-300 Da, while in PW streams the highest peaks were either discreetly distributed from 300 to 650 Da (i.e., P1) or concentrated between 480−510 Da (i.e., P2). This mass distribution difference, however, was not shown in the M_w/M_n ratio, which showed similar values for samples at T_0 (Table 3).

3.3.3 Van Krevelen Analysis

In DOM from FW streams, lignin-like components were the primary constituent, accounting for 78%−79% of molecules, and other biochemical class each comprised <10% of DOM molecules (Figure 4a, Table 4). Duplicate compounds of F1 and F2 (i.e., compounds existing in both F1 and F2) accounted for the majority of compounds in both F1 and F2 (i.e., 70%

for F1 and 84% for F2), which is in agreement with the great similarity between F1 *vs.* F2 (Table 2). Both duplicate compounds and unique compounds (i.e., compounds only in F1 or F2) were composed of primarily lignin-like components, i.e., 81% in duplicate compounds and 68%−72% in unique compounds. Relative to unique compounds in F1, those in F2 were characterized by higher proportions of condensed aromatic structures but lower proportions of protein-like components.

Table 3. Molecular Weight of DOM from FW and PW streams.

Incubation	**Time Point**	$\mathbf{M_n}$	$\mathbf{M_w}$	$\mathbf{M_w/M_n}$
F1 Bacteria-only	T_0	381.983540	401.575641	1.05
	T_{15}	384.209201	404.283618	1.05
F2 Bacteria-only	T_0	383.331089	407.260457	1.06
	T_{15}	391.708910	409.051912	1.04
P1 Bacteria-only	T_0	374.457707	398.211599	1.06
	T_{15}	408.455214	420.560807	1.03
P2 Bacteria-only	T_0	410.435600	430.779794	1.05
	T_{15}	416.718129	434.495434	1.04
F1 Light-only	T_0	384.475196	406.265320	1.06
	T_{15}	397.697685	414.414227	1.04
P1 Bacteria+light	T_0	374.457707	398.211599	1.06
	T_{15}	361.705312	381.103742	1.05
P2 Bacteria+light	T_0	410.435600	430.779794	1.05
	T_{15}	421.535378	437.202739	1.04

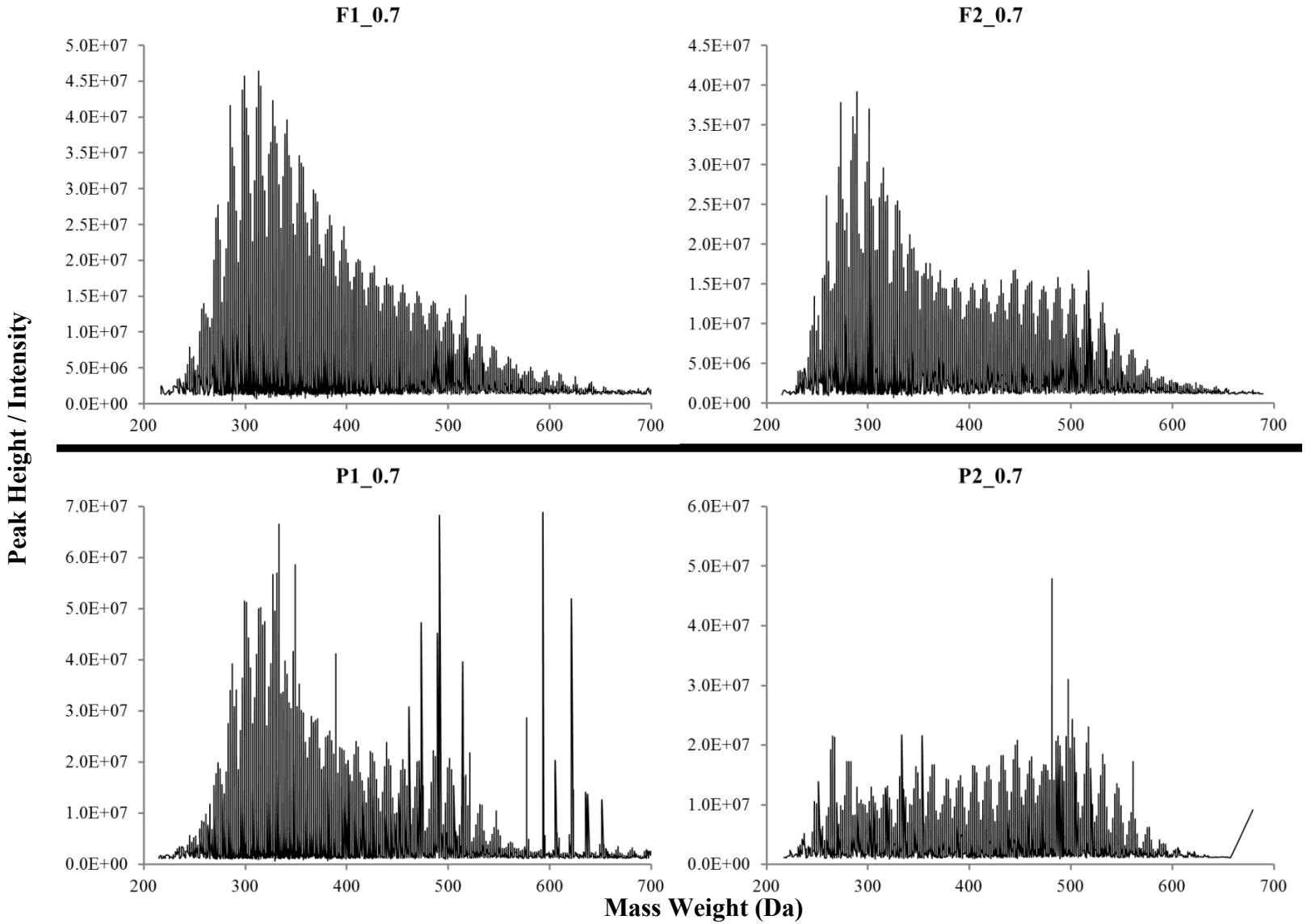

Figure 3. FTICRMS Ion chromatogram of streamwater DOM from the FW and PW streams at T_0. Peaks shown in the figures represent the DOM molecules assigned with formulae. F1 and F2 had highest peaks concentrated in the range of 280-300 Da, while the highest peaks were discretely distributed from 300 to 650 Da in P1 and concentrated between 480−510 Da in P2.

Table 4. The percentages of the six biochemical classes in DOM from FW and PW streams at T_0.

Sample ID	Total Numbers of Peaks	$(DBE)_w$*	$(O/C)_w$*	$(H/C)_w$*		Sum Identified	Lipid-like Components	Protein-like Components	Lignin-like Components	Carbohydrate-like Components	Unsaturated Hydrocarbon-like Components	Condensed Aromatic Structure-like Components
F1	3083	12.42	0.34	1.25	#	3077	154	189	2400	1	134	199
					%	99.81%	5.00%	6.13%	77.85%	0.03%	4.35%	6.45%
F2	2576	13.08	0.35	1.20	#	2575	115	84	2034	0	99	243
					%	99.96%	4.46%	3.26%	78.96%	0.00%	3.84%	9.43%
P1	2506	10.95	0.31	1.35	#	2501	359	194	1793	4	134	17
					%	99.80%	14.33%	7.74%	71.55%	0.16%	5.35%	0.68%
P2	1938	10.33	0.38	1.40	#	1936	278	259	1340	29	19	11
					%	99.90%	14.34%	13.36%	69.14%	1.50%	0.98%	0.57%

*The magnitude-averaged O/C ($(O/C)_w$), the magnitude-averaged H/C ($(H/C)_w$), and the magnitude-averaged double bond equivalent ($(DBE)_w$)values for each sample can be determined by the following formulae (Sleighter and Hatcher, 2008):$(O/C)_w=\sum(O/C_n\times M)$; $(H/C)_w=\sum(H/C_n\times M)$; $(DBE)_w=\sum(DBE\times M)$; where *w* signifies a magnitude-weighted calculation, n signifies that the parameter is calculated for each assigned molecular formula, and M is the relative magnitude of each peak.

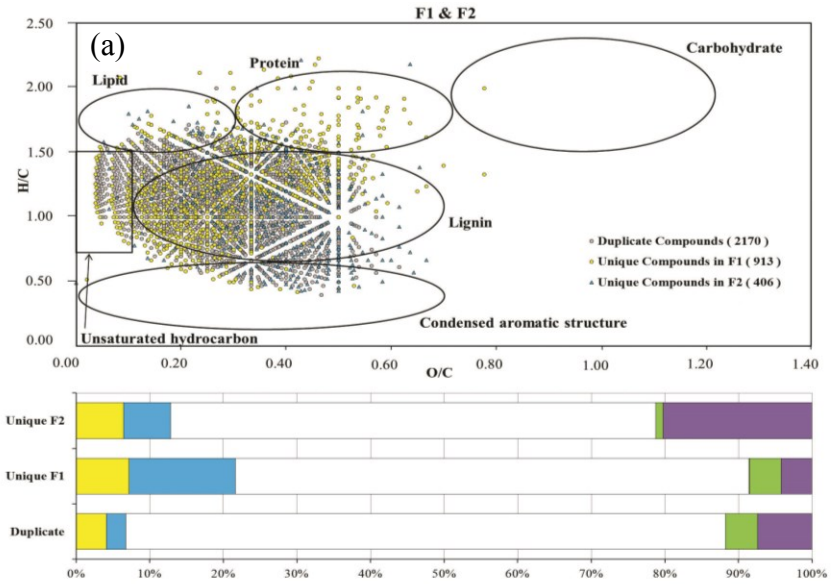
F1 & F2
(a)
Protein
Lipid
Carbohydrate
Lignin
Condensed aromatic structure
Unsaturated hydrocarbon
Duplicate Compounds (2170)
Unique Compounds in F1 (913)
Unique Compounds in F2 (406)
H/C
O/C
Unique F2
Unique F1
Duplicate

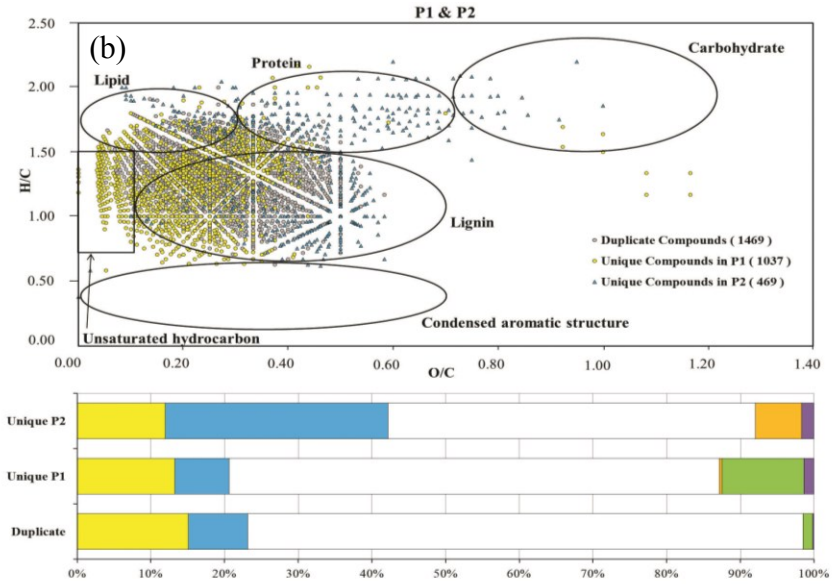
P1 & P2
(b)
Protein
Lipid
Carbohydrate
Lignin
Condensed aromatic structure
Unsaturated hydrocarbon
Duplicate Compounds (1469)
Unique Compounds in P1 (1037)
Unique Compounds in P2 (469)
H/C
O/C
Unique P2
Unique P1
Duplicate

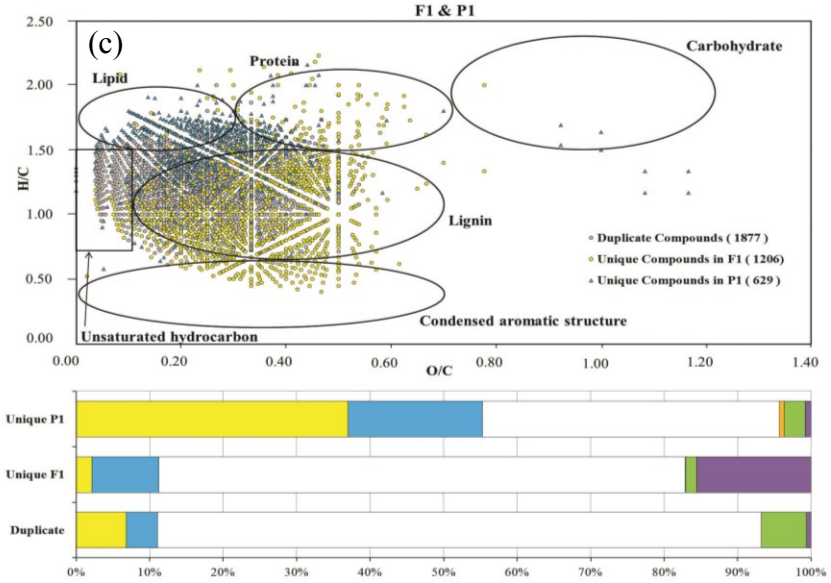
F1 & P1
(c)
Protein
Lipid
Carbohydrate
Lignin
Condensed aromatic structure
Unsaturated hydrocarbon
Duplicate Compounds (1877)
Unique Compounds in F1 (1206)
Unique Compounds in P1 (629)
H/C
O/C
Unique P1
Unique F1
Duplicate

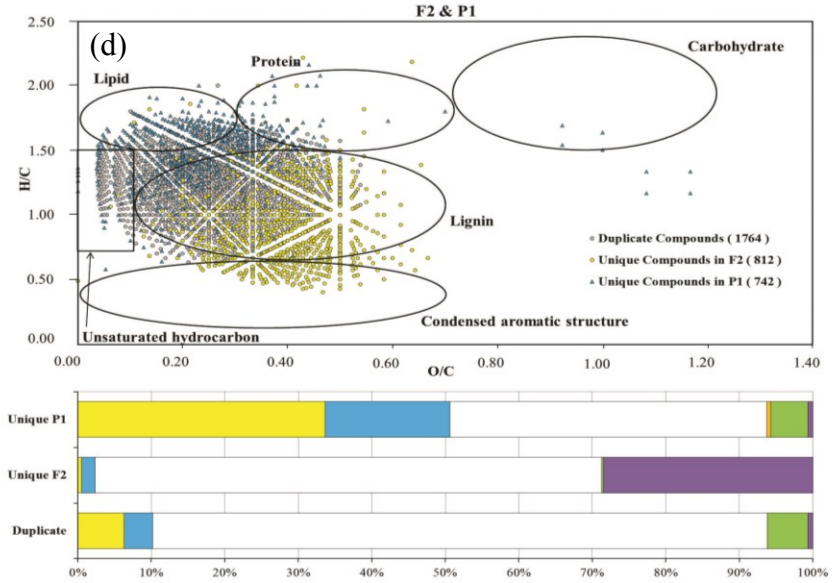
F2 & P1
(d)
Protein
Lipid
Carbohydrate
Lignin
Condensed aromatic structure
Unsaturated hydrocarbon
Duplicate Compounds (1764)
Unique Compounds in F2 (812)
Unique Compounds in P1 (742)
H/C
O/C
Unique P1
Unique F2
Duplicate

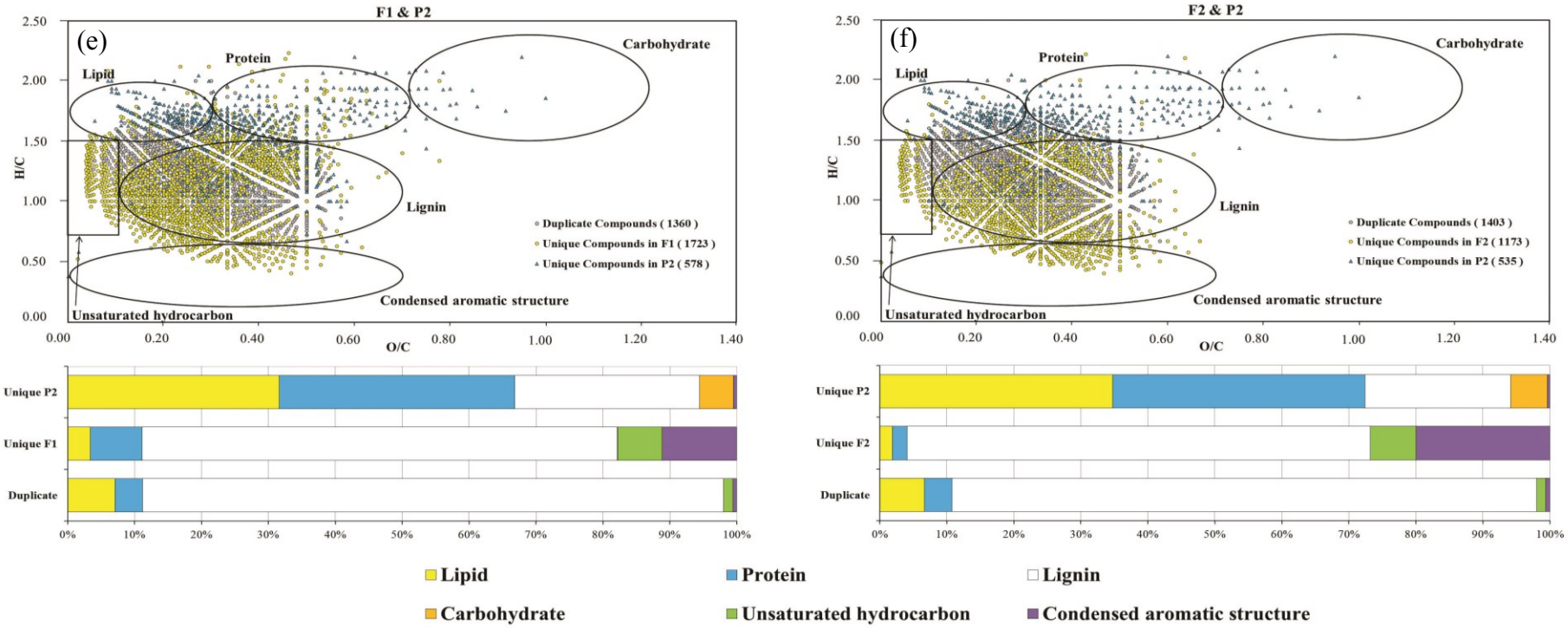

Figure 4. Comparison of DOM from FW *vs.* PW streams at T_0 in Van Krevelen diagrams. The bar plots below the Van Krevelen diagrams show the proportions of six biochemical classes in duplicate compounds (compounds appearing in both samples) and unique compounds (compounds appearing in only one of the two samples).

DOM of PW streams at T_0 contained primarily lignin-like components (69%−71%), which were similar to FW streams, but comprised greater relative abundance of lipid-like components (14%) and protein-like components (7%−13%) than FW streams (4%–5% lipid-like components, 3%–6% protein-like components; Table 4). Duplicate compounds of P1 and P2 accounted for 61% of the DOM compounds in P1 and 75% of the compounds in P2 (Figure 4b). These duplicate compounds were mainly composed of lignin-like components (75%), lipid-like components (15%) and protein-like components (8%). Unique components of these two streams comprised 31%−37% lipid-like components, 21%−43% lignin-like components and 16%−38% protein-like components. Compared with the unique compounds in P1, those in P2 were more enriched in protein-like components and carbohydrate-like components but less enriched in unsaturated hydrocarbon-like components.

As for the comparison between DOM compounds from FW streams and PW streams (Figures 4b-4f), duplicate compounds accounted for 44%−68% of DOM molecules of FW streams and 70%−75% of DOM molecules of PW streams. In the duplicate compounds, lignin-like components were the most abundant class (82%−88%), followed by lipid-like components (~7%) and protein-like components (~4%) (Figures 4c-4f and Appendix A).

It thus becomes clear that lignin-like components were the dominant class in all our samples. Lignin is found in the cell wall of vascular plants and makes an important component of decomposed terrestrial plants (Kogel-Knabner, 2002; Bianchi and Canuel, 2011). The predominance of lignin-like components we observed agrees with the previous observation that DOM in headwater streams is mostly allochothonous (Aitkenhead-Peterson et al., 2003; Williams et al., 2010; Lambert et al., 2011).

The unique compounds of FW streams had greater relative abundance of lignin-like

components but lower relative abundance of lipid-like components and protein-like components than those of PW streams (Figures 4c-4f and Appendix A). These results are consistent with those from a companion study of our study site, where excitation-emission matrix fluorescence combined with parallel factor analysis (EEM-PARAFAC) characterization of DOM showed that DOM of FW streams was characterized by greater percentages of terrestrial humic and terrestrial fulvic fluorescence but lower percentages of protein fluorescence relative to DOM of PW streams. (Lu et al., 2013). The agreement between molecular and fluorescence data shows that the fluorescent DOM, which only accounts for a fraction of DOM, is capable of providing reliable information about the sources of whole DOM pool. In addition, our results demonstrate that lignin-like components were the compound class primarily responsible for the greater humic and fulvic fluorescence in FW streams than in PW streams.

The relative abundance of protein-like components and lipid-like components in DOM reveal differences in the sources and reactivity of DOM between FW streams *vs*. PW streams. Proteins or amino acids are synthesized by fauna and flora, accounting for approximately ~22% of dissolved organic carbon in aquatic system and about 85% of the N in marine organisms (Bauer and Bianchi, 2011; Bianchi and Canuel, 2011). The abundance of free amino acids produced by proteins through hydrolysis is believed to be a proxy indicating the importance of proteins in supporting bacterial growth, controlling the activity of heterotrophic microbes and the flux of DOM in aquatic system (Kirchman, 2003). Relative to proteins, lipids are less abundant in aquatic systems (Bauer and Bianchi, 2011). Lipids are defined as all substances produced by organisms that are effectively insoluble in water (Bauer and Bianchi, 2011). In DOM, the major lipid class is fatty acid, which is an important cell membrane component and serves as an energy reserve for animals; hydrocarbons and sterols represent minor fractions of dissolved lipids

(Bianchi and Canuel, 2011). Lipids and proteins are overall more enriched in animals and bacterial than in terrestrial plants. The greater proportions of lipid-like components and protein-like components in the PW streams than in the FW streams indicates that the former was more influenced by autochthonous organic matter which may be attributed to the inputs of cattle wastes and/or associated *in situ* responses of microbes. Likewise, Wilson and Xenopoulos (2008) found that %croplands in watersheds were positively correlated to the relative amount of DOM with lower structural complexity and aromaticity, which are the general characteristics of DOM from algal and bacterial sources.

The larger relative abundance of lipid-like components and protein-like components in DOM of PW streams than in DOM of the FW streams implies that the former was more bioreacitve than the latter, on the basis that proteins and lipids are generally more bioreactive than lignins, unsaturated hydrocarbons and condensed aromatic structures (Kirchman, 2003; Baldock et al., 2004). Results from bioassay support the reactivity of protein for aquatic bacterial utilization. Harvey et al. (2006) collected water samples from the Chesapeake Bay, lower Delaware bay and freshwater marshes and enriched these samples with bovine serum albumin (a type of protein concentrate) before 48-hour dark incubations. Relative to the control samples without substrate addition, the protein treated samples showed larger bacterial cell volume detected by fluorescence *in situ* hybridization (FISH).

However, it is important to note that the bioreactivity of DOM is influenced by factors other than its chemical makeup. For example, molecular size influences the efficiency of bacteria utilization of DOM because that cell membrane cannot transport DOM > 600 amu (Weiss et al., 1991) and that large DOM has to be hydrolyzed by cell-associated extracellular enzymes (ectoenzymes) before its being efficiently utilized by heterotrophic bacteria (Kirchman et al.,

2004). Therefore, ectoenzymes and associated DOM hydrolysis could play an important role in the DOM bioreactivity and bacterial growth. Kirchman et al. (2004) collected water samples of Hudson River from north of Albany to New York City. Through inoculums experiments, they examined the effect of DOM on activity of ectoenzymes, bacterial growth and community structures by using FISH and fluorescent methylumbelliferone. Relative to inorganic nutrients, they found that DOM was more important in determining bacteria (e.g., ectoenzyme activity and the relative abundance of major heterotrophic bacterial groups), i.e., bacteria from the Albany site with greater %terrestrial DOM, showed stronger metabolic activity than that from the New York City site where lower %terrestrial DOM was found.

3.3.4 Index Analysis

DOM from FW streams at T_0 contained 24%−26% of aromatic compounds (AI > 0.5), 9%−13% of aliphatic compounds, 6%−9% of compounds with condensed aromatic ring structure, 5%−9% of black carbon-like components and 37%−43% of carboxyl-rich alicyclic molecule-like components (Figure 5 and Appendix B). By comparison, DOM from PW streams at T_0 contained 24%−31% of aliphatic compounds, 7%−12% of aromatic compounds, 0.8%−2% of compounds with condensed aromatic ring structure, 0.7%−0.9% of black carbon-like components and 31%−43% of carboxyl-rich alicyclic molecule-like components (Figure 5).

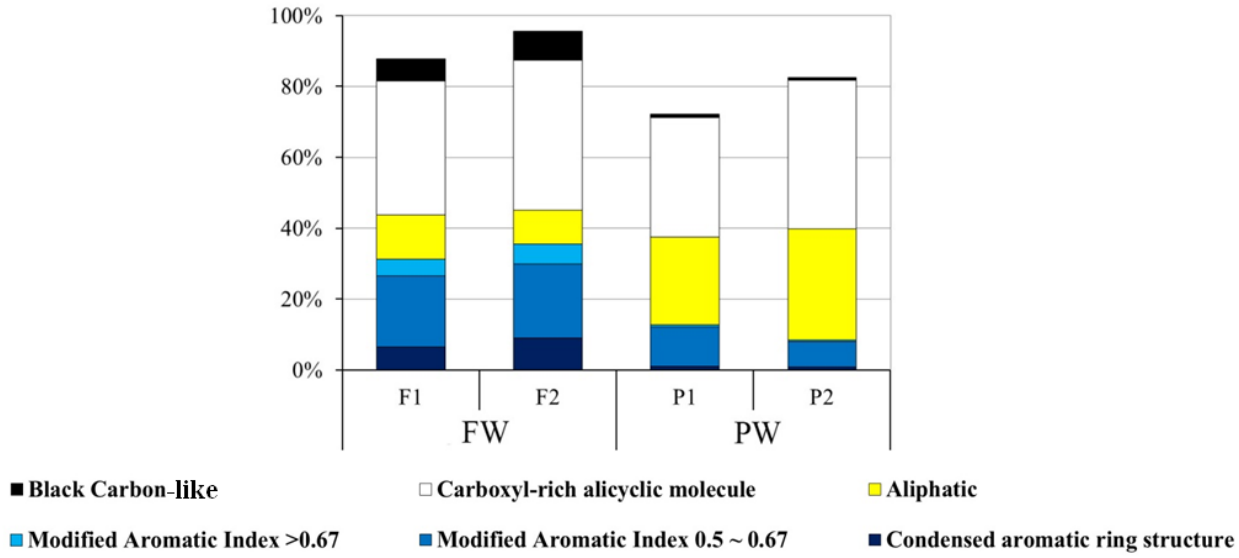

Figure 5. Comparison of DOM from FW *vs.* PW streams by index analysis at T_0. Note that the values of bars are less than 100% because 1) some molecules cannot be identified by the indices, and/or 2) the indices may identify the same molecules.

Relative to PW samples at T_0, FW samples contained greater proportions of aromatic compounds, condensed aromatic structure-like components, and had greater $(DBE)_w$ values (12.34−13.08) (Table 4). This difference in DOM may be related to variation in the sources and removal of DOM. Decomposition of forest litter has been observed to produce water soluble, lignin-derived aromatic compounds, which may contribute to the greater relative amounts of aromatic compounds in DOM of FW streams (Kalbitz et al., 2000; Kalbitz et al., 2006). Additionally, light penetration to PW streams may be greater than to FW streams due to removal of riparian trees in some sections of PW streams (field observation). Since light preferentially alters and remineralizes aromatic carbons with relative high DBE (Sulzberger and Durisch-Kaiser, 2009; Williams et al., 2010), it is unsurprising that PW streams contained lower amounts of aromatic compounds than FW streams.

The influence of agricultural land use on DOM structures remains inconclusive because variable patterns have been shown as to how agricultural land use alters DOM structural

complexity and aromaticity. Similar to the present study, Wilson and Xenopoulos (2009) and Williams et al. (2010) observed decreases in DOM aromaticity and structural complexity due to agricultural land use. Wilson and Xenopoulos (2009) measured DOM fluorescence to understand variability of streamwater DOM from 34 watersheds along a gradient of %cropland within draining watersheds in Canada. These studies found that aromaticity and the structural complexity of DOM decreased with increasing %cropland and decreasing %wetland in the draining watershed. Some other studies, however, have shown contrasting patterns (Sachse et al., 2005; Petrone et al., 2011), i.e., streamwater DOM with high structural complexity was related to agricultural catchments. Graeber et al. (2012) suggested that DOM structures may be influenced by a variety of watershed parameters in addition to land use, such as catchment size, agricultural management (e.g. fertilization, irrigation), soil type (e.g. bog, fen, forested wetland), and land use history (the land use type prior to the present land use). As such, it is unsurprising that variable influences of agricultural land use on DOM structures were observed.

The greater relative abundances of black carbon-like components (charcoal) and condensed aromatic ring structure in FW streams than in PW streams should also receive attention (Figure 5). Black carbon, or charcoal, is produced by incomplete combustion of biomass and fossil fuel (Goldberg, 1985) and may be a source of molecules with condensed aromatic structures (Cope, 1979; Baldock and Smernik, 2002; Kim et al., 2004; Hockaday et al., 2006; Hockaday et al., 2007). Hockaday et al. (2007) employed FTICR-MS to characterize DOM leached from soil charcoal particles from a forested watershed impacted by fire. They found that condensed aromatic ring structures accounted for 65% of identified DOM molecules and had exact masses and empirical formulae similar to the majority of condensed aromatic ring structures detected in pore water and streamwater DOM in an adjacent forested watershed.

Further, previous study indicated that black carbon oxidation in soils may trigger the export of black carbon from soils to surface water DOM pool (Hockaday et al., 2006). During the process of photochemical and biological degradation, polar functional groups (i.e. hydroxyl groups) can be added to aromatic rings, increasing the solubility of the aromatic compounds and resulting in the solubilization of black carbon degradation products (Kim et al., 2004). Therefore, the greater abundance of black carbon-like components and condensed aromatic structure-like components in DOM form FW streams than from PW streams could be related to the controlled fire in the forested watersheds to stimulate forest growth.

3.4 Comparison of DOM Compounds prior to and after Bacterial Transformation

3.4.1 DOM Composition Similarity

The jaccard similarity coefficients of FW streams, i.e., 0.754 for F1 at T_0 and T_{15} and 0.653 for F2 at T_0 and T_{15} (Table 5), demonstrate that DOM of FW streams was similar before vs. after the bacterial incubations. In contrast, the low jaccard similarity coefficients for PW streams, 0.260 for P1 at T_0 and T_{15} and 0.445 for P2 at T_0 and T_{15}, indicate that DOM was altered by bacteria. This observation supports our postulation based on DOM molecular composition – DOM from PW streams was more bioreactive than DOM form FW streams. Likewise, Williams et al. (2010) observed that microbial activity indicated by extracelluar leucine aminopeptidase activity bacterial production was higher in streams influenced by agricultural land use than in pristine streams.

3.4.2 Mass Distribution

After the bacteria-only incubations, M_w and M_n values of all the samples increased, while only no or little difference was detected for the ratios of M_w/M_n (i.e., 0.00 for F1, 0.02 for F2, 0.03 for P1 and 0.01 for P2), suggesting that bacterial processing had little influence on the mass

distribution of DOM (Table 3).

3.4.3 Van Krevelen Analysis

We compared the compounds prior to *vs.* after the bacterial incubations and identified three compound groups: 1) refractory compounds that did not change during the incubations and thus existed at both T_0 and T_{15}; 2) reactive compounds referring to the compounds existing only at T_0 because they were remineralized or altered over the course of incubations; and 3) products referring to the compounds existing only at T_{15} because they were produced by bacteria.

Table 5. Comparison of DOM components from FW and PW streams prior to and after the bacteria-only incubations.

Sample & Incubation Type	Time Point	Total Numbers of Peaks	Precent Reactive DOC (%)*	$(DBE)_w$	$(O/C)_w$	$(H/C)_w$	Refractory Components		Reactive Components		Products		Jaccard Similarity Coefficient
							#Peaks	%	#Peaks	%	#Peaks	%	
F1 Bacteria-only	T_0	3083	13.2	12.42	0.34	1.25	2642	85.70%	441	14.30%	-	-	0.754
	T_{15}	3063		12.69	0.35	1.24	2642	86.26%	-	-	421	13.74%	
F2 Bacteria-only	T_0	2576	15.0	13.08	0.35	1.20	2036	79.04%	540	20.96%	-	-	0.653
	T_{15}	2576		12.17	0.39	1.21	2036	79.04%	-	-	540	20.96%	
P1 Bacteria-only	T_0	2506	1.9	10.95	0.31	1.35	802	32.00%	1704	68.00%	-	-	0.260
	T_{15}	1386		9.47	0.41	1.38	802	57.86%	-	-	584	42.14%	
P2 Bacteria-only	T_0	1938	23.9	10.33	0.38	1.40	1350	69.66%	588	30.34%	-	-	0.445
	T_{15}	2449		11.29	0.38	1.30	1350	55.12%	-	-	1099	44.88%	

*Data source: Lu et al., 2013.

The refractory components accounted for 79%−86% of DOM compounds in FW streams and 32%−70% in PW streams. In refractory compounds of FW samples, 80%−82% were lignin-like components, 6%−9% were condensed aromatic structure-like components, and 3%−5% were unsaturated hydrocarbon-like components (Figures 5a, 5b and Appendix C). In the refractory compounds of PW streams, 74%−80% were lignin-like components, 10%−15% were lipid-like components and 9%−11% were protein-like components (Figures 5c, 5d). In the reactive components, the three main biochemical classes from FW streams were lignin-like components (63%−70%), condensed aromatic structure-like components (6%−13%) and lipid-like components (8%−11%); while the three main classes of DOM from the PW streams were lignin-like components (57%−68%), lipid-like components (14%−17%) and protein-like components (6%−22%).

After the bacterial incubations, the products made up 14%−21% of DOM compounds in FW samples but 42%−45% in PW samples. The products included lignin-like components (71%−80%), protein-like components (11%−16%) and condensed aromatic structure-like components (4%−6%) for FW streams and included lignin-like components (64%−77%), protein-like components (8%−25%) and lipid-like components (5%−6%) for PW streams.

The changes in the proportions of biogeochemical classes in DOM were small (up to 2%) for both FW streams (Figures 5a, 5b and Table 6), agreeing with the high values of jaccard similarity coefficients between T_0 vs. T_{15} samples. By comparison, the changes in the proportions of biogeochemical classes in DOM of P1 and P2 were different (e.g., the proportion of protein-like components increased by 8% in P1 but decreased by 4.25%) in P2 (Figures 5c, 5d and Table 6). This observation is expected given the dissimilarity of P1 and P2 prior to the incubation (Table 2 and Figure 4b).

Table 6. The abundance of the six biochemical classes in DOM from FW and PW streams prior to and after the bacteria-only incubations.

Sample ID	Time Point		Sum Identified	Lipid-like Components	Protein-like Components	Lignin-like Components	Carbohydrate-like Components	Unsaturated Hydrocarbon-like Components	Condensed Aromatic Structure-like Components
F1 Bacteria-only	T_0	#	3077	154	189	2400	1	134	199
		%	99.81%	5.00%	6.13%	77.85%	0.03%	4.35%	6.45%
	T_{15}	#	3062	122	185	2420	4	138	193
		%	99.97%	3.98%	6.04%	79.01%	0.13%	4.51%	6.30%
F2 Bacteria-only	T_0	#	2575	115	84	2034	0	99	243
		%	99.96%	4.46%	3.26%	78.96%	0.00%	3.84%	9.43%
	T_{15}	#	2573	82	121	2086	1	84	199
		%	99.88%	3.18%	4.70%	80.98%	0.04%	3.26%	7.73%
P1 Bacteria-only	T_0	#	2501	359	194	1793	4	134	17
		%	99.80%	14.33%	7.74%	71.55%	0.16%	5.35%	0.68%
	T_{15}	#	1383	117	228	1015	3	15	5
		%	99.78%	8.44%	16.45%	73.23%	0.22%	1.08%	0.36%
P2 Bacteria-only	T_0	#	1936	278	259	1340	29	19	11
		%	99.90%	14.34%	13.36%	69.14%	1.50%	0.98%	0.57%
	T_{15}	#	2447	249	223	1848	1	23	103
		%	99.92%	10.17%	9.11%	75.46%	0.04%	0.94%	4.21%

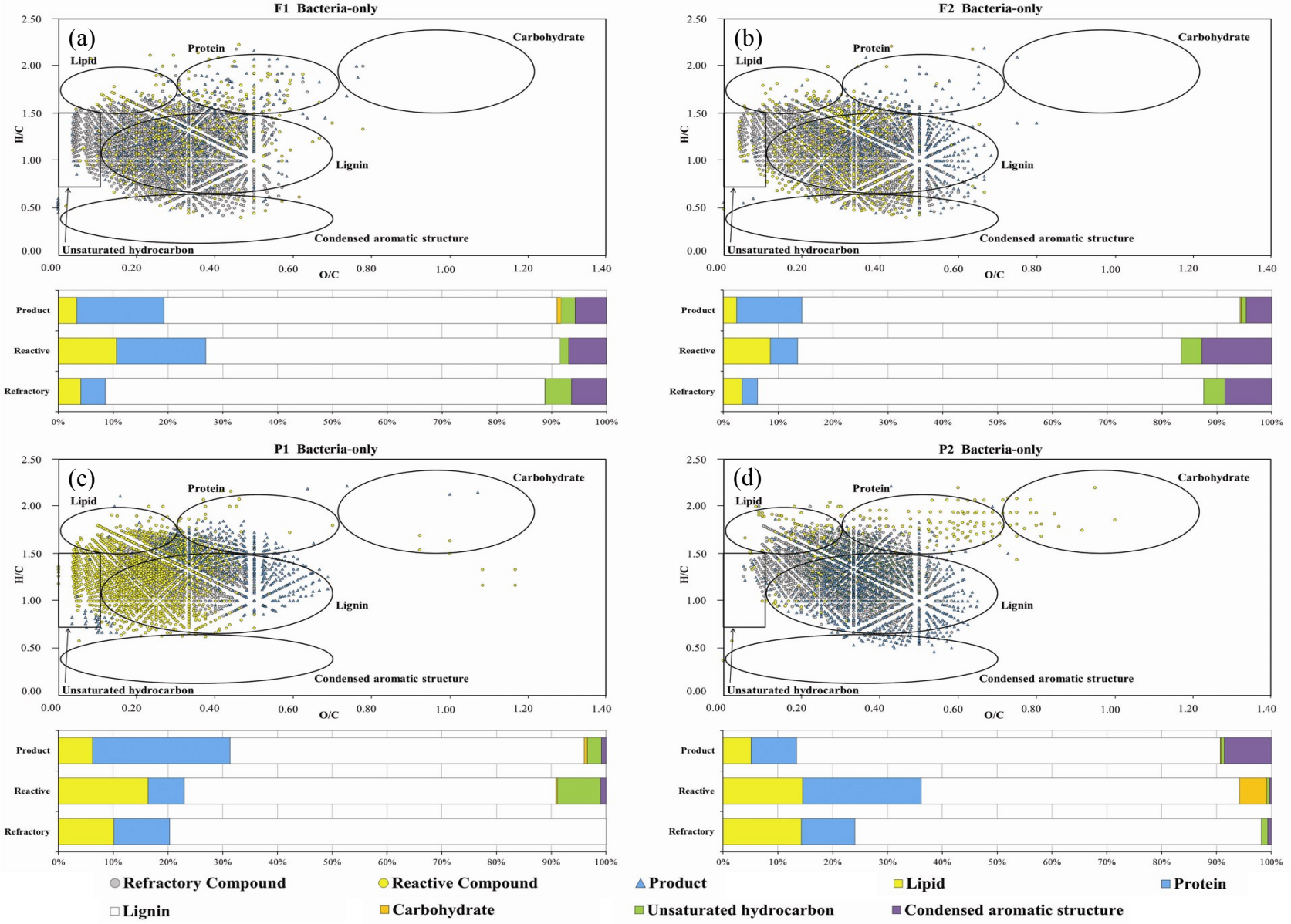

Figure 6. Comparison of DOM from FW and PW streams prior to and after bacteria-only incubations in Van Krevelen diagrams. The bar plots below the Van Krevelen diagrams show the proportions of six biochemical classes in refractory compounds (compounds appearing in samples at T_0 and T_{15}), reactive compounds (compounds appearing only in samples at T_0) and product (compounds appearing only in samples at T_{15}).

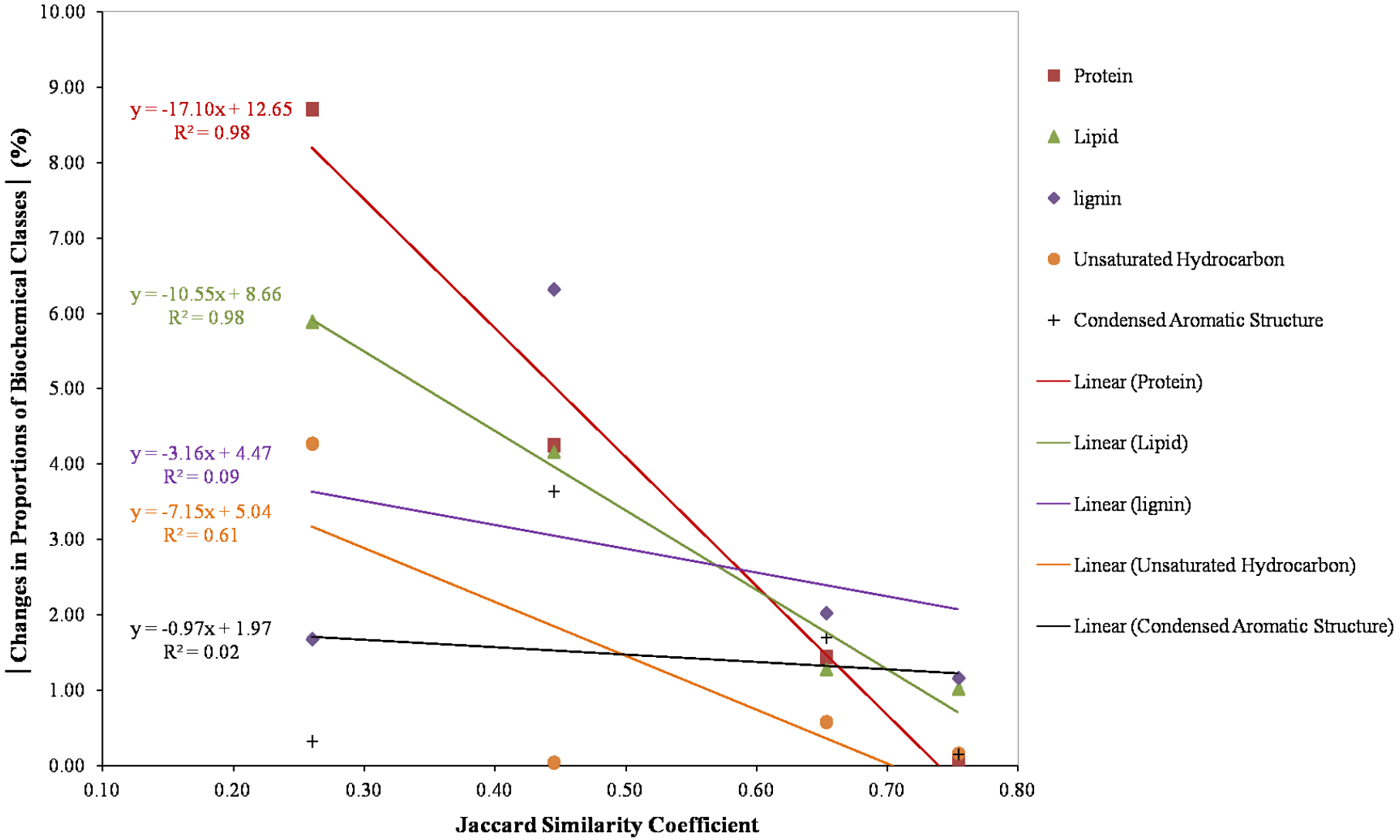

Figure 7. Correlation between jaccard similarity coefficients and absolute changes in the proportions of six biochemical classes associated with the bacteria-only incubations. The changes in %protein-like components, %lipid-like components and %unsaturated hydrocarbon-like components show strong correlation with the Jaccard Similarity Coefficients, indicating these three classes are primarily responsible for the changes in DOM molecular compositions.

Both FW and PW samples showed that bacterial transformation reduced the proportions of lipid-like components but increased the proportions of lignin-like components (Table 6), which indicates that lipid is a bioreactive class while lignin is refractory to bacterial processing. The degradation of lipids has been observed in many previous studies (Harvey and Macko, 1997; Goutx et al., 2003; Kalbitz et al., 2003; Christodoulou et al., 2009). For example, Kalbitz et al. (2003) conducted 90-day bacterial incubations of DOM from forest soils, peats, and agricultural soils, where they found a relative decrease of lipids in DOM. Harvey and Macko (1997) conducted oxic and anoxic experiments for two kinds of phytoplankton (diatom and cyanobacterium) in Chesapeake Bay water to compare the degradation rate of lipid components during microbially mediated decay. They found that unsaturated constituents of lipids degraded more rapidly than saturated constituents and fatty acids decreased more significantly under oxic conditions than anoxic conditions.

On the basis of jaccard similarity coefficients, the extent of DOM alteration during bacterial incubations was in the order of F1<F2<P2<P1 (Table 5). The same order was observed for the changes in the proportion of protein-like components: F1 (changed by 0.09%)<F2 (1.44%)<P2 (4.25%)<P1 (8.71%)(Table 6). Moreover, among the six biogeochemical classes, the changes in the proportions of protein-like components was best correlated with jaccard similarity coefficients (Figure 7 R^2=0.98), which indicates that a greater degree of changes in DOM molecules corresponds to a larger change in %protein-like components. Similar relationships were found for lipid-like components and unsaturated hydrocarbon-like components but not for lignin-like components and condensed aromatic structure-like components (carbohydrate-like components were not plotted because of the low abundance of these compounds). This observation suggests that protein-like components, lipid-like

components and unsaturated hydrocarbon-like components were the biochemical classes primarily responsible for the changes in DOM under the influences of bacterial processing. Several previous studies have found a general positive correlation between the abundance of protein fluorescence and %biodegradable DOC and therefore suggested that the former may potentially serve as predictor of the latter (Balcarczyk et al., 2009; Fellman et al., 2009). Such a correlation, however, was not found in our study streams (Lu et al., 2013), and can be explained by the molecular analysis here –lipid-like components and unsaturated hydrocarbon-like components also play an important part in determining the DOC bioreactivity in our samples.

Notably, the molecular analysis here showed that 68% of initial DOM in P1 was altered by bacteria processing (Table 5), which is in distinct contract to only 1.9% of DOC of P1 being remineralized by bacteria (Lu et al., 2013). Therefore, although bacteria did not completely remove DOM through remineralization, they were actively transforming DOM compounds. As such, %degradable DOC, a proxy easy to measure and therefore commonly used to indicate DOM bioreactivity (e.g., Lu et al., 2013), is not a reliable indicator to reflect the amount of DOM being transformed/utilized by microbes. The combination of DOM molecules and microbial measurements (e.g., enzymes, sequence analysis) should be used to assess the quality of DOM in supporting microbial food webs.

3.4.4 Index Analysis

The indices showed that the two FW samples had similar changes during the bacterial incubations. Both samples showed ≤3% decreases in the relative abundance of aromatic compounds, aliphatic compounds, compounds with condensed aromatic ring structure, as well as black carbon-like components and ≤3% increases in carboxyl-rich alicyclic molecule-like components (Figures 8a, 8b and Appendix D). The two PW samples, however, showed different

changes (Figures 8c, 8d). Aromatic compounds decreased by 9% in P1 but increased by 8% in P2; compounds with condensed aromatic ring structure decreased by <1% in P1 but increased by 3% in P2; aliphatic compounds increased by <1% in P1 but decreased by 10% in P2; black carbon-like components decreased by <1% in P1 but increased by 3% in P2; the relative abundance of carboxyl-rich alicyclic molecule-like components increased by 19% in P1 but only 4% in P2.

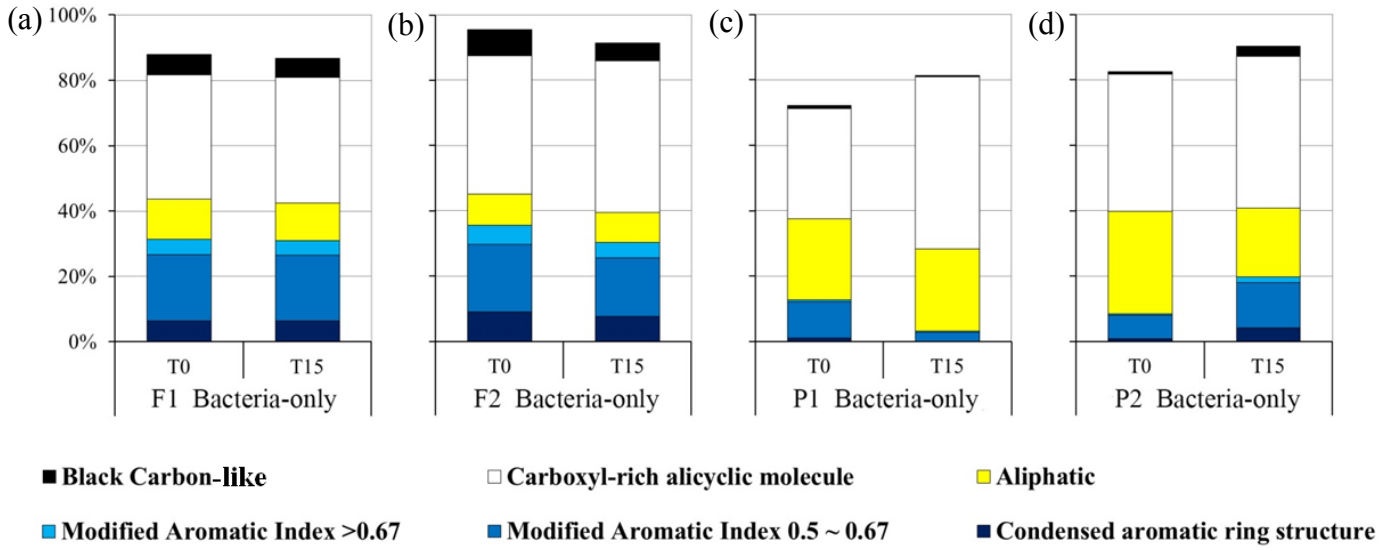

Figure 8. Comparison of DOM from FW and PW streams prior to and after bacterial-only incubations by index analysis. Note that the values of bars less than 100% are due that 1) some molecules are unidentified by indices, and/or 2) the indices may identify the same molecules.

One common pattern shared by the FW and PW samples is that the proportions of carboxyl-rich alicyclic molecule-like components increased after the bacterial incubations (Figures 8a-8d and Appendix D). Carboxyl-rich alicyclic molecules were thought to contain mainly the decomposition products of biomolecules (Hertkorn et al., 2006). As a refractory component of DOM, they are particularly abundant in the deep ocean (Hertkorn et al., 2006; Lam et al., 2007). The increases in carboxyl-rich alicyclic molecule-like components observed

here may be a combined result of the production of these molecules from bacterial decomposition of lipid-like components and protein-like components and the refractory nature of these molecules.

In P2, the proportion of black carbon-like components DOM increased after bacteria-only incubation. Since there is no known pathway where bacteria produce black carbon, to our knowledge, this observation may be due to the bias from the index-defined black carbon ($0.3<O/C<0.6$, $H/C<0.8$).

3.5 Comparison of DOM Compounds prior to and after the Light-only and Bacteria+light Incubations

3.5.1 DOM Composition Similarity

F1 at T_0 shared less similarity with F1 at T_{15} after the light-only incubation (0.222, Table 7) than with F1 at T_{15} after bacterial-only incubation (0.754, Table 5), indicating photochemical processing had a greater influence on DOM than bacterial processing. This observation agrees with that a greater amount of DOC was removed (50.0%, Table 7) by light than by bacteria (13.2%, Table 5) (Lu et al., 2013).

The jaccard similarity coefficients for PW streams associated with bacterial+light incubations (0.267 for P1 at T_0 and T_{15} and 0.465 for P2 at T_0 and T_{15}) demonstrated that DOM in PW samples was significantly altered during bacterial+light incubations and that the degree of DOM alteration in P1 was greater than P2 (Table 7). These alterations were larger than those associated with bacteria-only incubations.

3.5.2 Mass Distribution

The changes in the ratios of M_w/M_n were small, suggesting that molecular mass distribution did not change apparently during light-only or light+bacteria incubations (Table 3).

Table 7. Comparison of DOM components from FW and PW streams prior to and after the light-only and bacteria+light incubations.

Sample & Incubation Type	Time Point	Total Numbers of Peaks	Precent Reactive DOC (%)*	$(DBE)_w$	$(O/C)_w$	$(H/C)_w$	Refractory Components		Reactive Components		Products		Jaccard Similarity Coefficient
							#Peaks	%	#Peaks	%	#Peaks	%	
F1 Light-only	T_0	2899	50.5	12.34	0.34	1.27	888	30.63%	2011	69.37%	-	-	0.222
	T_{15}	1983		11.02	0.46	1.32	888	44.78%	-	-	1095	55.22%	
P1 Bacteria+light	T_0	2506	15.9	10.95	0.31	1.35	674	26.90%	1832	73.10%	-	-	0.267
	T_{15}	692		8.12	0.34	1.41	674	97.40%	-	-	18	2.60%	
P2 Bacteria+light	T_0	1938	50.0	10.33	0.38	1.40	1223	63.11%	715	36.89%	-	-	0.465
	T_{15}	1916		9.58	0.41	1.39	1223	63.83%	-	-	693	36.17%	

* Data source: Lu et al., 2013.

Table 8. The abundance of the six biochemical classes in DOM from FW streams and PW streams prior to and after light-only and bacteria+light incubations.

Sample ID	Time Point		Sum Identified	Lipid-like Components	Protein-like Components	Lignin-like Components	Carbohydrate-like Components	Unsaturated Hydrocarbon-like Components	Condensed Aromatic Structure-like Components
F1 Light-only	T_0	#	2891	206	187	2108	19	159	212
		%	99.72%	7.11%	6.45%	72.71%	0.66%	5.48%	7.31%
	T_{15}	#	1970	54	178	1651	55	10	22
		%	99.34%	2.72%	8.98%	83.26%	2.77%	0.50%	1.11%
P1 Bacteria+light	T_0	#	2501	359	194	1793	4	134	17
		%	99.80%	14.33%	7.74%	71.55%	0.16%	5.35%	0.68%
	T_{15}	#	690	101	82	495	0	12	0
		%	99.71%	14.60%	11.85%	71.53%	0.00%	1.73%	0.00%
P2 Bacteria+light	T_0	#	1936	205	142	1517	4	48	20
		%	99.90%	10.58%	7.33%	78.28%	0.21%	2.48%	1.03%
	T_{15}	#	1915	211	158	1480	5	24	37
		%	99.95%	11.01%	8.25%	77.24%	0.26%	1.25%	1.93%

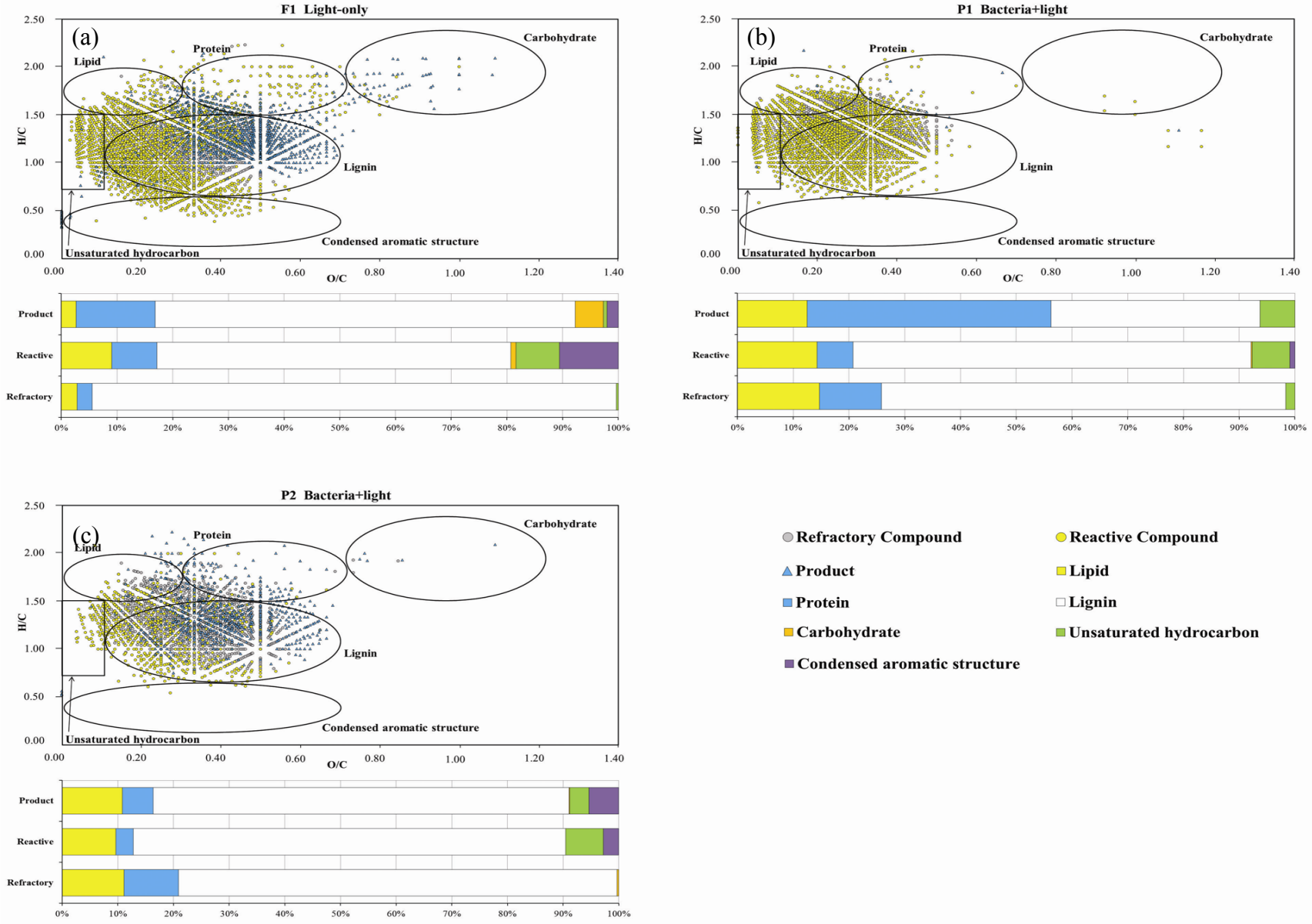

Figure 9. Comparison of DOM from FW and PW streams prior to and after light-only and bacteria+light incubations in Van Krevelen diagrams**.** The bar plots below the Van Krevelen diagrams show the proportions of six biochemical classes in refractory compounds (compounds appearing in samples at T_0 and T_{15}), reactive compounds (compounds appearing only in samples at T_0) and product (compounds appearing only in samples at T_{15}).

3.5.3 Van Krevelen Analysis

Based on the Van Krevelen analysis, lignin-like components, lipid-like components and protein-like components accounted for 94%, 3% and 3% of refractory compounds of F1 samples, respectively (Figure 9a). However, lignin-like components, lipid-like components and protein-like components constituted 72%−79%, 11%−15%, 9%−11% of refractory compounds in PW samples, respectively (Figures 9b, 9c). In F1 samples, the reactive compounds included lignin-like components (63%), condensed aromatic structure-like components (11%) and lipid-like components (9%). In PW samples, the reactive compounds included mainly lignin-like components (71%−77%), lipid-like components (9%−14%) and unsaturated hydrocarbon-like components (6%−7%). The products of F1 samples included lignin-like components (75%), protein-like components (14%) and carbohydrate-like components (5%), but the products of P1 and P2 samples included lignin-like components (33%−75%), protein-like components (5%−14%) and lipid-like components (10%−11%).

Three common patterns were observed for the changes in the three DOM samples after the light-only and bacteria+light incubations. First, the proportions of protein-like components increased (Table 8), which may be due that light could stimulate autochthonous production of protein-like components as observed in Williams et al. (2010). Second, we observed increases in $(O/C)_w$ for all the three samples (Table 7). Similarly, Kujawinski et al. (2004) irradiated DOM samples from Suwannee river with light of wavelengths >305 and >360 nm and found that DOM compounds with high DBE and low oxygen content were generally destroyed, leaving behind DOM compounds with low DBE and high oxygen content. Increased oxygen content in DOM after photochemical transformation has been repeatedly observed (Schmitt-Kolpin et al., 1998; Kujawinski et al., 2004; Gonsior et al., 2009; Stubbins et al., 2010), which is consistent with the

proposed DOM photochemical oxidation pathways—DOM ionization by light may yield hydrated electrons and organic radical that both can react with molecular oxygen, leading to the addition of oxygen to DOM (Sulzberger and Durisch-Kaiser, 2009). Lastly, we found the decreases in unsaturated hydrocarbon-like components and $(DBE)_w$, which is expected as unsaturated bonds (e.g., C=C, benzene rings, conjugate systems) are sensitive to light alterations.

In sample F1, the percent reactive DOC during the bacteria+light incubations streams (91.5±0.9%) was greater than the sum of percent reactive bioreactive DOC (13.2±1.6%) and the percent reactive photoreactive DOC (50.5±1.4%) (Lu et al., 2013). The molecular data presented here may provide an explanation for this observation—photochemical alterations increased the amounts of bioreactive carbohydrate-like components but decreased the amount of condensed aromatic structure-like components (Table 8) and thereby enhanced the bioreactivey of DOM. Similarly, Obernosterer and Benner (2004) found that 22% of reactive DOC for biomineralization is contributed by photochemical products. By altering DOM into smaller oxygen-rich organic compounds such as carbohydrate-like components and inorganic carbon (e.g., CO and CO_2) that may serve as the food source for heterotrophic bacteria and autotrophic bacteria, respectively, sunlight may enhance the bioavailability of DOM (Moran and Zepp, 1997; Sulzberger and Durisch-Kaiser, 2009). Counter to this view, photochemical transformation of DOM can hamper DOM bioavailability (review by Sulzberger and Durisch-Kaiser, 2009 and references therein). Light may promote the formation of biorecalcitrant compounds and decrease the bioavailability of DOM (Sulzberger and Durisch-Kaiser, 2009). For example, Moran and Zepp (1997) explained that CO produced during DOM photochemical mineralization may not be utilized efficiently at the concentrations found in surface waters on the basis that the microbial turnover time of CO (e.g., 20−250 h) is much longer the residence time of CO in marine and

freshwater environments (e.g., 3−4h).

3.5.4 Index Analysis

Comparing the samples prior to and after light-present incubations (Figures 10a-10c and Appendix D), we found that in F1 samples, the proportions of aromatic compounds, black carbon-like components, condensed aromatic ring structure and aliphatic compounds decreased by 21 %, 7%, 7%, 1%, respectively, but carboxyl-rich alicyclic molecule-like components increased by 26%. In P1 and P2 samples, the proportions of aromatic compounds, condensed aromatic ring structure and black carbon-like components decreased by 6%−11%,<1%, <1% but carboxyl-rich alicyclic molecule-like components increased by 11% after bacteria+light incubations. The aliphatic compounds in PW streams increased by 5% in P1 but decreased by 7% in P2.

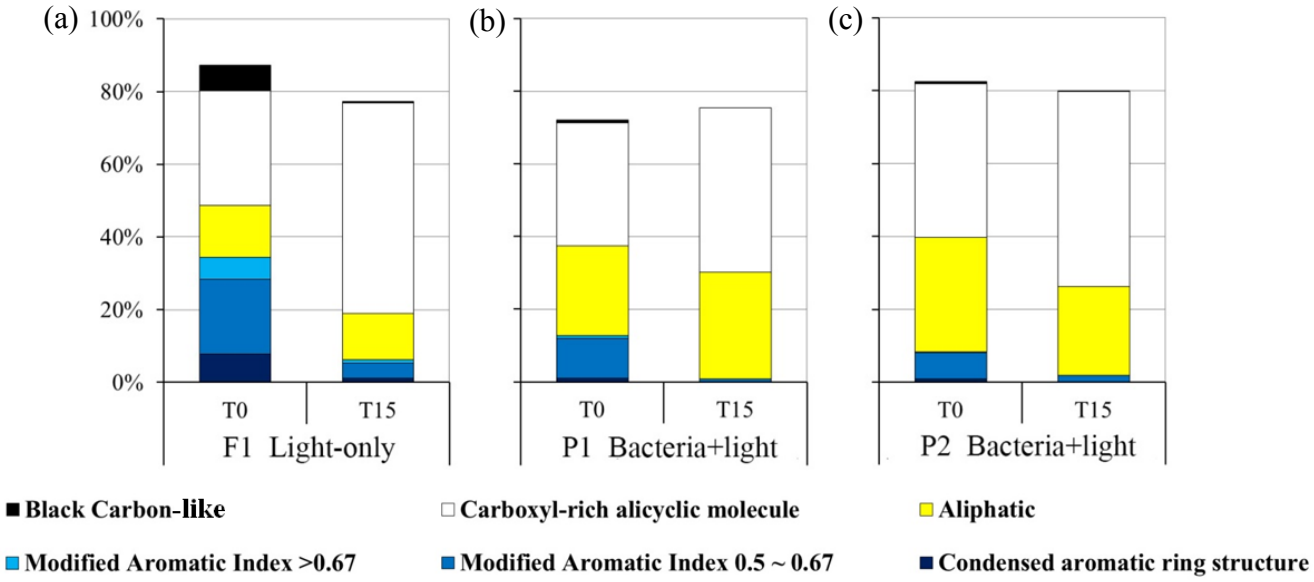

Figure 10. Comparison of DOM from FW and PW streams prior to and after the light-only and bacteria+light incubations by index analysis. Note that the values of bars less than 100% are due that 1) some molecules are unidentified by indices, and/or 2) the indices may identify the same molecules.

A common pattern shared by the three samples after light-present incubations is that the proportions of aromatic compounds, and condensed aromatic ring structure decreased but carboxyl-rich alicyclic molecule-like components increased. Similar results have been shown for photochemical transformation of DOM from the Congo River, where the proportions of aromatic compounds (AI>0.5) and black carbon-like components condensed aromatic ring structure decreased (Stubbins et al., 2010). Dalzell et al. (2009) utilized high performance size exclusion chromatography, temperature-resolved MS and ESI-MS to assess estuarine DOM photochemical transformation. Their results showed that light preferentially altered upstream DOM which is more aromatic and contains greater % terrestrially-derived materials than downstream samples.

Interestingly, the majority of dissolved black carbon-like components was removed during the light-only and bacteria+light incubations (Figures 10a-10c). Dissolved black carbon, widely observed in aquatic environment (Dittmar, 2008; Jaffe et al., 2013), has been considered stable due to its abundant content of aromatic and graphitic C (Major et al., 2009). However, black carbon is not inert because it plays many important roles in soil formation, fertility and pollutant availability (Hockaday et al., 2006; Jaffe et al., 2013). The decomposition rate of black carbon also has been evidenced as faster than previously estimated (Hockaday et al., 2007; Jaffe et al., 2013). For instance, Kim et al. (2004) identified hydrogen-deficient molecules (low H/C ratio, less than 1) in riverine DOM from the McDonalds branch (New Jersey, USA) and considered them oxidation products of black carbon, suggesting that black carbon may be degraded in the environment and play an active part in global carbon cycling. Furthermore, Dittmar (2008) utilized high-performance liquid chromatography to determine black carbon in marine DOM from the Gulf of Mexico by quantifying benzenepolycarboxylic acids (BPCAs), the product of black carbon oxidation by nitric acid. He detected BPCAs in all marine water

samples and found that black carbon decreased from near-shore to offshore waters from 2.6% to 0.9% of DOC. Therefore, these studies substantiate our finding that dissolved black carbon-like components was reactive to photochemical oxidations.

CHAPTER 4

CONCLUSIONS

Through the use of ESI-FTICR-MS, we compared DOM from streams draining forest-dominated watersheds *vs.* DOM from streams draining pasture-dominated watersheds with respect to molecular composition and molecular transformation associated with photochemical and microbial processes. Results can be summarized into three main findings:

First, DOM molecular composition differed between the two land use types, reflecting the differences in the sources and input of DOM. Although lignin-like components dominated in all samples, which indicates the predominance of terrestrial DOM in both types of streams, DOM from FW streams is characterized by higher proportions of condensed aromatic molecules and greater structural complexity but lower proportions of protein-like components and lipid-like components than PW streams. This difference may be attributed to the lower inputs of decomposed high plant litters in pasture watersheds than in forest watersheds. The abundance of black carbon-like components in FW streams was relatively greater than PW streams, which may be associated with controlled fire to stimulate forest growth in forested watersheds. Further, the similarity of DOM components between F1 and F2 samples was greater than between P1 and P2 samples, presumably due to greater difference in the percentages of land use cover between P1 and P2.

Second, watershed land use may influence DOM microbial reactivity, i.e., the degree of changes in DOM molecular composition under the influences of bacterial processing. DOM of PW streams showed greater degrees of changes than DOM of FW streams after the bacterial

incubations, and that protein-like components, lipid-like components and unsaturated hydrocarbon-like components are the biochemical classes primarily responsible for the changes associated with bacterial processing of DOM. This finding is also consistent with the inferred differences in DOM bioreactivity between FW *vs.* PW streams from the initial DOM molecular composition, i.e., greater relative abundance of bioreactive classes (lipid-like components and protein-like components) was observed in PW streams than in FW streams.

Third, DOM of FW and PW streams shared similar behavior under the influence of bacterial and photochemical processes, providing information about the reactivities of different biochemical classes. The proportions of lipid-like components decreased but the proportions of carboxyl-rich alicyclic molecule-like components and lignin-like components increased after the bacteria-only incubations. The light-only and bacterial+light incubations increased the relative abundance of carboxyl-rich alicyclic molecule-like components as well as the proportions of protein-like components but reduced the proportions of dissolved black carbon-like components. These observations suggest that carboxyl-rich alicyclic molecule-like components are refractory to both photochemical and bacterial alteration while lignin-like components are resistant to bacterial alteration. Protein-like components and dissolved black carbon-like components are reactive to photochemical and bacterial transformation respectively.

Collectively, this study demonstrates that human land use in upstream watersheds may alter the molecular composition of streamwater DOM as well as its behaviors to photochemical and microbial processing. These alterations not only impact the biological role of DOM in upstream ecosystems but also potentially change the characteristics of DOM reaching downstream rivers, estuaries and coastal oceans.

REFERENCES

Aitkenhead-Peterson J.A., McDowell W.H. & Neff J.C. (2003). Sources, Production, and Regulation of Allochthonous Dissolved Organic Matter Inputs to Surface Waters. In *Aquatic Ecosystems: Interactivity of Dissolved Organic Matter* (edited by Findlay S. E. G. and Sinsabaugh R. L.). Academic Press.

Aufdenkampe A.K., Mayorga E., Raymond P.A., Melack J.M., Doney S.C., Alin S.R., Aalto R.E. & Yoo K. (2011). Riverine coupling of biogeochemical cycles between land, oceans, and atmosphere. *Frontiers in Ecology and the Environment,* **9,** 53-60.

Balcarczyk K.L., Jones Jr. J.B., Jaffé R. & Maie N. (2009). Stream dissolved organic matter bioavailability and composition in watersheds underlain with discontinuous permafrost. *Biogeochemistry,* **94,** 255-270.

Baldock J.A., Masiello C.A., Gelinas Y. & Hedges J.I. (2004). Cycling and composition of organic matter in terrestrial and marine ecosystems. *Marine Chemistry,* **92,** 39-64.

Baldock J.A. & Smernik R.J. (2002). Chemical composition and bioavailability of thermally altered Pinus resinosa (Red pine) wood. *Organic Geochemistry,* **33,** 1093-1109.

Bauer J.E. & Bianchi T.S. (2011). Dissolved Organic Carbon Cycling and Transformation. In *Treatise on Estuarine and Coastal Science.* ScienceDirect, EBSCOhost.

Benner R. (2003). Molecular Indicators of the Bioavailability of Dissolved Organic Matter. In *Aquatic Ecosystems: Interactivity of Dissolved Organic Matter* (edited by Findlay S. E. G. and Sinsabaugh R. L.). Academic Press.

Bertilsson S. & Jones J.B. (2003). Supply of Dissolved Organic Matter to Aquatic Ecosystems. Autochthonous Sources. In *Aquatic Ecosystems: Interactivity of Dissolved Organic Matter* (edited by Findlay S. E. G. and Sinsabaugh R. L.). Academic Press.

Bianchi T.S., DiMarco S.F., Cowan J.H., Hetland R.D., Chapman P., Day J.W. & Allison M.A. (2010). The science of hypoxia in the Northern Gulf of Mexico: A review. *Science of the Total Environment,* **408,** 1471-1484.

Bianchi T.S. & Canuel E.A. (2011). *Chemical biomarkers in aquatic ecosystems.* Princeton : Princeton University Press.

Chin Y., Aiken G. & O'Loughlin E. (1994). Molecular weight, polydispersity, and spectroscopic properties of aquatic humic substances. *Environmental Science and Technology,* **28,** 1853-1858.

Christodoulou S., Rontani J., Marty J., Miquel J. & Volkman J.K. (2009). Use of lipids and their degradation products as biomarkers for carbon cycling in the northwestern Mediterranean Sea. *Marine Chemistry,* **113,** 25-40.

Clair T.A., Dennis I.F. & Vet R. (2011). Water chemistry and dissolved organic carbon trends in lakes from Canada's Atlantic Provinces: No recovery from acidification measured after 25 years of lake monitoring. *Canadian Journal of Fisheries and Aquatic Sciences,* **68,** 663-674.

Clark J.M., Bottrell S.H., Evans C.D., Monteith D.T., Bartlett R., Rose R., Newton R.J. & Chapman P.J. (2010). The importance of the relationship between scale and process in understanding long-term DOC dynamics. *Science of the Total Environment,* **408,** 2768-2775.

Cole J.J. & Caraco N.F. (2001). Carbon in catchments: connecting terrestrial carbon losses with aquatic metabolism. *Marine and Freshwater Research,* **52,** 101-110.

Cooper A.R. (1989). *Determination of molecular weight*. New York : J. Wiley, 1989.

Cope M.J. (1980). Physical and chemical properties of coalified and charcoalified phytoclasts from some British Mesozoic sediments: An organic geochemical approach to palaeobotany. *Physics and Chemistry of the Earth,* **12,** 663-677.

Dalzell B.J., Minor E.C. & Mopper K.M. (2009). Photodegradation of estuarine dissolved organic matter: a multi-method assessment of DOM transformation. *Organic Geochemistry,* **40,** 243-257.

Dalzell B.J., Minor E.C. & Mopper K.M. (2009). Photodegradation of estuarine dissolved organic matter: a multi-method assessment of DOM transformation. *Organic Geochemistry,* **40,** 243-257.

Dittmar T. (2008). The molecular level determination of black carbon in marine dissolved organic matter. *Organic Geochemistry,* **39,** 396-407.

Fellman J.B., Hood E., Edwards R.T. & D'Amore D.V. (2009). Changes in the concentration, biodegradability, and fluorescent properties of dissolved organic matter during stormflows in coastal temperate watersheds. *Journal of Geophysical Research: Biogeosciences,* **114,** G01021, DOI: 10.1029/2008JG000790.

Foley J.A., DeFries R., Asner G.P., Barford C., Bonan G., Carpenter S.R., Chapin F.S., Coe M.T., Daily G.C., Gibbs H.K., Helkowski J.H., Holloway T., Howard E.A., Kucharik C.J., Monfreda C., Patz J.A., Prentice I.C., Ramankutty N. & Snyder P.K. (2005). Global consequences of land use. *Science,* **309,** 570-574.

Gennings C., Molot L.A. & Dillon P.J. (2001). Enhanced photochemical loss of organic carbon in acidic waters. *Biogeochemistry,* **52,** 339-354.

Goldberg E.D. (1985). *Black carbon in the environment: properties and distribution*. John Wiley and Sons, New York, NY.

Gonsior M., Peake B.M., Cooper W.J., Cooper W.T., Podgorski D. & D'Andrilli J. (2009). Photochemically induced changes in dissolved organic matter identified by ultrahigh resolution fourier transform ion cyclotron resonance mass spectrometry. *Environmental Science and Technology,* **43,** 698-703.

Goutx M., Guigue C. & Striby L. (2003). Triacylglycerol biodegradation experiment in marine environmental conditions: Definition of a new lipolysis index. *Organic Geochemistry,* **34,** 1465-1473.

Graeber D., Gelbrecht J., Pusch M.T., Anlanger C. & von Schiller D. (2012). Agriculture has changed the amount and composition of dissolved organic matter in Central European headwater streams. *Science of the Total Environment,* **438,** 435-446.

Harvey H.R., Dyda R.Y. & Kirchman D.L. (2006). Impact of DOM composition on bacterial lipids and community structure in estuaries. *Aquatic Microbial Ecology,* **42,** 105-117.

Harvey H.R. & Macko S.A. (1997). Kinetics of phytoplankton decay during simulated sedimentation: Changes in lipids under oxic and anoxic conditions. *Organic Geochemistry,* **27,** 129-140.

Hertkorn N., Benner R., Frommberger M., Schmitt-Kopplin P., Witt M., Kaiser K., Kettrup A. & Hedges J.I. (2006). Characterization of a major refractory component of marine dissolved organic matter. *Geochimica et Cosmochimica Acta,* **70,** 2990-3010.

Hockaday W.C., Grannas A.M., Kim S. & Hatcher P.G. (2006). Direct molecular evidence for the degradation and mobility of black carbon in soils from ultrahigh-resolution mass spectral analysis of dissolved organic matter from a fire-impacted forest soil. *Organic Geochemistry,* **37,** 501-510.

Hockaday W.C., Purcell J.M., Marshall A.G., Baldock J.A. & Hatcher P.G. (2009). Electrospray and photoionization mass spectrometry for the characterization of organic matter in natural waters: a qualitative assessment. *Limnology and Oceanography-Methods,* **7,** 81-95.

Hockaday W.C., Grannas A.M., Kim S. & Hatcher P.G. (2007). The transformation and mobility of charcoal in a fire-impacted watershed. *Geochimica et Cosmochimica Acta,* **71,** 3432-3445.

Jaffé R., Ding Y., Niggemann J., Vähätalo A.,V., Stubbins A., Spencer R.G.M., Campbell J. & Dittmar T. (2013). Global charcoal mobilization from soils via dissolution and riverine transport to the oceans. *Science (New York, N.Y.),* **340,** 345-347.

Kalbitz K., Kaiser K., Bargholz J. & Dardenne P. (2006). Lignin degradation controls the production of dissolved organic matter in decomposing foliar litter. *European Journal of Soil Science,* **57,** 504-516.

Kalbitz K., Schmerwitz J., Schwesig D. & Matzner E. (2003). Biodegradation of soil-derived dissolved organic matter as related to its properties. *Geoderma,* **113,** 273-291.

Kalbitz K., Solinger S., Park J.H., Michalzik B. & Matzner E. (2000). Controls on the dynamics of dissolved organic matter in soils: A review. *Soil Science,* **165,** 277-304.

Kim S., Kaplan L.A., Benner R. & Hatcher P.G. (2004). Hydrogen-deficient molecules in natural riverine water samples - evidence for the existence of black carbon in DOM. *Marine Chemistry,* **92,** 225-234.

Kim S., Kaplan L.A. & Hatcher P.G. (2006). Biodegradable dissolved organic matter in a temperate and a tropical stream determined from ultra-high resolution mass spectrometry. *Limnology and Oceanography,* **51,** 1054-1063.

Kim S., Kramer R.W. & Hatcher P.G. (2003b). Graphical Method for Analysis of Ultrahigh-Resolution Broadband Mass Spectra of Natural Organic Matter, the Van Krevelen Diagram. *Analytical Chemistry,* **75,** 5336-5344.

Kim S., Simpson A.J., Kujawinski E.B., Freitas M.A. & Hatcher P.G. (2003a). High resolution electrospray ionization mass spectrometry and 2D solution NMR for the analysis of DOM extracted by C 18 solid phase disk. *Organic Geochemistry,* **34,** 1325-1335.

Kirchman D.L. (2003). The Contribution of Monomers and other Low-Molecular Weight Compounds to the Flux of Dissolved Organic Material. In *Aquatic Ecosystems: Interactivity of Dissolved Organic Matter* (edited by S. E. G. Findlay, and R. L. Sinsabaugh). Academic Press.

Kirchman D.L., Dittel A.I., Findlay S.E.G. & Fischer D. (2004). Changes in bacterial activity and community structure in response to dissolved organic matter in the Hudson River, New York. *Aquatic Microbial Ecology,* **35,** 243-257.

Koch B.P. & Dittmar T. (2006). From mass to structure: An aromaticity index for high-resolution mass data of natural organic matter. *Rapid Communications in Mass Spectrometry,* **20,** 926-932.

Koch B.P., Dittmar T., Witt M. & Kattner G. (2007). Fundamentals of molecular formula assignment to ultrahigh resolution mass data of natural organic matter. *Analytical Chemistry,* **79,** 1758-1763.

Kogel-Knabner I. (2002). The macromolecular organic composition of plant and microbial residues as inputs to soil organic matter. *Soil Biology & Biochemistry,* **34,** 139-162.

Kujawinski E.B., Del Vecchio R., Blough N.V., Klein G.C. & Marshall A.G. (2004). Probing molecular-level transformations of dissolved organic matter: insights on photochemical degradation and protozoan modification of DOM from electrospray ionization Fourier transform ion cyclotron resonance mass spectrometry. *Marine Chemistry,* **92,** 23-37.

Kujawinski E.B. & Behn M.D. (2006). Automated analysis of electrospray ionization fourier transform ion cyclotron resonance mass spectra of natural organic matter. *Analytical Chemistry,* **78,** 4363-4373.

Lam B., Baer A., Simpson A.J., Alaee M., Lefebvre B., Moser A. & Williams A. (2007). Major structural components in freshwater dissolved organic matter. *Environmental Science and Technology,* **41,** 8240-8247.

Lambert T., Pierson-Wickmann A., Gruau G., Thibault J.N. & Jaffrezic A. (2011). Carbon isotopes as tracers of dissolved organic carbon sources and water pathways in headwater catchments. *Journal of Hydrology,* **402,** 228-238.

Lu Y., Bauer J.E., Canuel E.A., Yamashita Y., Chambers R.M. & Jaffé R. (2013). Photochemical and microbial alteration of dissolved organic matter in temperate headwater streams associated with different land use. *Journal of Geophysical Research: Biogeosciences,* **118,** 566-580.

Major J., Lehmann J., Rondon M. & Goodale C. (2010). Fate of soil-applied black carbon: downward migration, leaching and soil respiration. *Global Change Biology,* **16,** 1366-1379.

Mattsson T., Kortelainen P. & Räike A. (2005). Export of DOM from boreal catchments: Impacts of land use cover and climate. *Biogeochemistry,* **76,** 373-394.

McCallister S.L., Bauer J.E., Ducklow H.W. & Cherrier J.E. (2004). Assessing sources and ages of organic matter supporting river and estuarine bacterial production: A multiple-isotope (Δ14C, δ13C, and δ15N) approach. *Limnology and Oceanography,* **49,** 1687-1702.

Mopper K., Stubbins A., Ritchie J.D., Bialk H.M. & Hatcher P.G. (2007). Advanced Instrumental Approaches for Characterization of Marine Dissolved Organic Matter: Extraction Techniques, Mass Spectrometry, and Nuclear Magnetic Resonance Spectroscopy. *Chemical reviews,* **107,** 419-442.

Moran M.A. & Zepp R.G. (1997). Role of Photoreactions in the Formation of Biologically Labile Compounds from Dissolved Organic Matter. *Limnology and Oceanography,* **42,** 1307-1316.

Mosher J.J., Klein G.C., Marshall A.G. & Findlay R.H. (2010). Influence of bedrock geology on dissolved organic matter quality in stream water. *Organic Geochemistry,* **41,** 1177-1188.

Nebbioso A. & Piccolo A. (2013). Molecular characterization of dissolved organic matter (DOM): a critical review. *Analytical and Bioanalytical Chemistry,* **405,** 109-124.

Obernosterer I. & Benner R. (2004). Competition between biological and photochemical processes in the mineralization of dissolved organic carbon. *Limnology and Oceanography,* **49,** 117-124.

Ohno T., He Z., Honeycutt C.W., Sleighter R.L. & Hatcher P.G. (2010). Ultrahigh resolution mass spectrometry and indicator species analysis to identify marker components of soil- and plant biomass-derived organic matter fractions. *Environmental Science and Technology,* **44,** 8594-8600.

Parsons, T., Maita, Y., & Lalli, C. M. (1989). *A manual of chemical and biological methods for seawater analysis* (edited by Timothy R. Parsons, Yoshiaki Maita and Carol M. Lalli). Oxford ; New York : Pergamon Press, 1989, c1984.

Perdue E.M. (1984). Analytical constraints on the structural features of humic substances. *Geochimica et Cosmochimica Acta,* **48,** 1435-1442.

Petrone K.C., Donn M.J., Fellman J.B., Grierson P.F. & Hood E. (2011). The origin and function of dissolved organic matter in agro-urban coastal streams. *Journal of Geophysical Research: Biogeosciences,* **116,** G01028, doi:10.1029/2010JG001537.

Piccolo A. & Spiteller M. (2003). Electrospray ionization mass spectrometry of terrestrial humic substances and their size fractions. *Analytical and Bioanalytical Chemistry,* **377,** 1047-1059.

Sachse A., Gelbrecht J., Henrion R. & Steinberg C.E.W. (2005). Classification of dissolved organic carbon (DOC) in river systems: Influence of catchment characteristics and autochthonous processes. *Organic Geochemistry,* **36,** 923-935.

Schmitt-Kopplin P., Hertkorn N., Schulten H.R. & Kettrup A. (1998). Structural changes in a dissolved soil humic acid during photochemical degradation processes under O-2 and N-2 atmosphere. *Environmental science & technology,* **32,** 2531-2541.

Simjouw J., Minor E.C. & Mopper K. (2005). Isolation and characterization of estuarine dissolved organic matter: Comparison of ultrafiltration and C18 solid-phase extraction techniques. *Marine Chemistry,* **96,** 219-235.

Sleighter R.L. & Hatcher P.G. (2007). The application of electrospray ionization coupled to ultrahigh resolution mass spectrometry for the molecular characterization of natural organic matter. *Journal of Mass Spectrometry,* **42,** 559-574.

Sleighter R.L., McKee G.A., Liu Z. & Hatcher P.G. (2008). Naturally present fatty acids as internal calibrants for Fourier transform mass spectra of dissolved organic matter. *Limnology and Oceanography: Methods,* **6,** 246-251.

Sleighter R.L. & Hatcher P.G. (2008). Molecular characterization of dissolved organic matter (DOM) along a river to ocean transect of the lower Chesapeake Bay by ultrahigh resolution electrospray ionization Fourier transform ion cyclotron resonance mass spectrometry. *Marine Chemistry,* **110,** 140-152.

Spencer R.G.M., Wabakanghanzi J.N., Hernes P.J., Dyda R.Y., Stubbins A., Mopper K., Baker A., Aufdenkampe A.K., Mwamba V.L., Mangangu A.M. & Six J. (2009). Photochemical degradation of dissolved organic matter and dissolved lignin phenols from the Congo River. *Journal of Geophysical Research: Biogeosciences,* **114,** G03010, doi:10.1029/2009JG000968.

Stanley E.H., Powers S.M., Crawford J.T., Lottig N.R. & Buffam I. (2012). Contemporary changes in dissolved organic carbon (DOC) in human-dominated rivers: Is there a role for DOC management? *Freshwater Biology,* **57,** 26-42.

Stenson A.C., Marshall A.G. & Cooper W.T. (2003). Exact masses and chemical formulas of individual Suwannee River fulvic acids from ultrahigh resolution electrospray ionization Fourier transform ion cyclotron resonance mass spectra. *Analytical Chemistry,* **75,** 1275-1284.

Stubbins A., Chen H., Hatcher P.G., Mopper K., Spencer R.G.M., Six J., Hernes P.J., Mwamba V.L., Mangangu A.M. & Wabakanghanzi J.N. (2010). Illuminated darkness: Molecular signatures of Congo River dissolved organic matter and its photochemical alteration as revealed by ultrahigh precision mass spectrometry. *Limnology and Oceanography,* **55,** 1467-1477.

Sulzberger B. & Durisch-Kaiser E. (2009). Chemical characterization of dissolved organic matter (DOM): A prerequisite for understanding UV-induced changes of DOM absorption properties and bioavailability. *Aquatic Sciences,* **71,** 104-126.

Weiss M.S., Abele U., Weckesser J., Welte W., Schiltz E. & Schulz G.E. (1991). Molecular architecture and electrostatic properties of a bacterial porin. *Science,* **254,** 1627-1630.

Williams C.J., Xenopoulos M.A., Yamashita Y., Jaffe R. & Wilson H.F. (2010). Unraveling the role of land use and microbial activity in shaping dissolved organic matter characteristics in stream ecosystems. *Limnology and Oceanography,* **55,** 1159-1171.

Wilson H.F. & Xenopoulos M.A. (2009). Effects of agricultural land use on the composition of fluvial dissolved organic matter. *Nature Geoscience,* **2,** 37-41.

Zhong J., Sleighter R.L., Salmon E., McKee G.A. & Hatcher P.G. (2011). Combining advanced NMR techniques with ultrahigh resolution mass spectrometry: A new strategy for

molecular scale characterization of macromolecular components of soil and sedimentary organic matter. *Organic Geochemistry,* **42,** 903-916.

APPENDIX

Appendix A. Comparison of six biochemical classes in duplicate compounds and unique compounds of DOM at T_0 from FW streams and PW streams.

Sample ID	Compounds		Sum Identified	Lipid-like Components	Protein-like Components	Lignin-like Components	Carbohydrate-like Components	Unsaturated hydrocarbon-like Components	Condensed aromatic structure-like Components
F1&F2	Duplicate Compounds	#	2170	89	58	1767	0	95	161
		%	100.00%	4.10%	2.67%	81.43%	0.00%	4.38%	7.42%
	Unique Compounds in F1	#	913	65	131	633	1	39	38
		%	99.34%	7.12%	14.35%	69.33%	0.11%	4.27%	4.16%
	Unique Compounds in F2	#	406	26	26	267	0	4	82
		%	99.75%	6.40%	6.40%	65.76%	0.00%	0.99%	20.20%
P1&P2	Duplicate Compounds	#	1469	222	118	1107	0	19	3
		%	100.00%	15.11%	8.03%	75.36%	0.00%	1.29%	0.20%
	Unique Compounds in P1	#	1037	137	76	686	4	115	14
		%	99.52%	13.21%	7.33%	66.15%	0.39%	11.09%	1.35%
	Unique Compounds in P2	#	469	56	141	233	29	0	8
		%	99.57%	11.94%	30.06%	49.68%	6.18%	0.00%	1.71%
F1&P1	Duplicate Compounds	#	1877	128	80	1541	0	116	12
		%	100.00%	6.82%	4.26%	82.10%	0.00%	6.18%	0.64%
	Unique Compounds in F1	#	1206	26	109	859	1	18	187

		%	99.50%	2.16%	9.04%	71.23%	0.08%	1.49%	15.51%
	Unique Compounds in P1	#	629	231	114	252	4	18	5
		%	99.21%	36.72%	18.12%	40.06%	0.64%	2.86%	0.79%
F1&P2	Duplicate Compounds	#	1360	96	56	1181	0	19	8
		%	100.00%	7.06%	4.12%	86.84%	0.00%	1.40%	0.59%
	Unique Compounds in F1	#	1723	58	133	1219	1	115	191
		%	99.65%	3.37%	7.72%	70.75%	0.06%	6.67%	11.09%
	Unique Compounds in P2	#	578	182	203	159	29	0	3
		%	99.65%	31.49%	35.12%	27.51%	5.02%	0.00%	0.52%
F2&P1	Duplicate Compounds	#	1764	111	69	1475	0	97	12
		%	100.00%	6.29%	3.91%	83.62%	0.00%	5.50%	0.68%
	Unique Compounds in F2	#	812	4	15	559	0	2	231
		%	99.88%	0.49%	1.85%	68.84%	0.00%	0.25%	28.45%
	Unique Compounds in P1	#	742	248	125	318	4	37	5
		%	99.33%	33.42%	16.85%	42.86%	0.54%	4.99%	0.67%
F2&P2	Duplicate Compounds	#	1403	93	58	1224	0	19	9
		%	100.00%	6.63%	4.13%	87.24%	0.00%	1.35%	0.64%
	Unique Compounds in F2	#	1173	22	26	810	0	80	234
		%	99.91%	1.88%	2.22%	69.05%	0.00%	6.82%	19.95%
	Unique Compounds in P2	#	535	185	201	116	29	0	2
		%	99.63%	34.58%	37.57%	21.68%	5.42%	0.00%	0.37%

Appendix B. Percentages of DOM compounds from FW streams and PW streams at T_0 categorized by index analysis.

ID		Total	Sum Identified	CARS	Modified AI 0.5 ~ 0.67	Modified AI >0.67	Aliphatic	CRAM	Black carbon-like components
F1	#	3083	1941	199	767	146	382	1167	353
	%	100.00%	62.96%	6.45%	20.14%	4.74%	12.39%	37.85%	6.25%
F2	#	2576	1643	231	686	149	246	1090	392
	%	100.00%	63.78%	8.97%	20.85%	5.78%	9.55%	42.31%	8.12%
P1	#	2506	1589	26	291	15	622	846	68
	%	100.00%	63.41%	1.04%	11.01%	0.60%	24.82%	33.76%	0.87%
P2	#	1938	1441	16	146	6	608	816	43
	%	100.00%	74%	0.8%	7.2%	0.3%	31.4%	42.1%	0.7%

Appendix C. Comparison of six biochemical classes in refractory compounds, reactive compounds and products prior to and after bacteria-only, light-only, and bacteria+light incubations.

Sample ID	Compounds		Sum Identified	Lipid-like Components	Protein-like Components	Lignin-like Components	Carbohydrate-like Components	Unsaturated Hydrocarbon-like Components	Condensed Aromatic Structure-like Components
F1 Bacteria-only	Refractory	#	2642	108	118	2119	1	127	169
		%	100.00%	4.09%	4.47%	80.20%	0.04%	4.81%	6.40%
	Reactive	#	441	46	71	281	0	7	30
		%	98.64%	10.43%	16.10%	63.72%	0.00%	1.59%	6.80%
	Product	#	421	14	67	301	3	11	24
		%	99.76%	3.33%	15.91%	71.50%	0.71%	2.61%	5.70%
F2 Bacteria-only	Refractory	#	2036	69	57	1657	0	79	174
		%	100.00%	3.39%	2.80%	81.39%	0.00%	3.88%	8.55%
	Reactive	#	540	46	27	377	0	20	69
		%	99.81%	8.52%	5.00%	69.81%	0.00%	3.70%	12.78%
	Product	#	540	13	64	429	1	5	25
		%	99.44%	2.41%	11.85%	79.44%	0.19%	0.93%	4.63%
P1 Bacteria-only	Refractory	#	802	81	82	639	0	0	0
		%	100.00%	10.10%	10.22%	79.68%	0.00%	0.00%	0.00%
	Reactive	#	1704	278	112	1154	4	134	17
		%	99.71%	16.31%	6.57%	67.72%	0.23%	7.86%	1.00%
	Product	#	584	36	146	376	3	15	5
		%	99.49%	6.16%	25.00%	64.38%	0.51%	2.57%	0.86%
P2 Bacteria-only	Refractory	#	1350	193	132	1000	0	16	9
		%	100.00%	14.30%	9.78%	74.07%	0.00%	1.19%	0.67%

	Reactive	#	588	85	127	340	29	3	2
		%	99.66%	14.46%	21.60%	57.82%	4.93%	0.51%	0.34%
	Product	#	1099	56	91	848	1	7	94
		%	99.82%	5.10%	8.28%	77.16%	0.09%	0.64%	8.55%
F1 Light-only	Refractory	#	888	25	24	834	0	3	0
		%	99.77%	2.82%	2.70%	93.92%	0.00%	0.34%	0.00%
	Reactive	#	2011	181	163	1274	19	156	212
		%	99.70%	9.00%	8.11%	63.35%	0.94%	7.76%	10.54%
	Product	#	1095	29	154	817	55	7	22
		%	99.00%	2.65%	14.06%	74.61%	5.02%	0.64%	2.01%
P1 Bacteria+light	Refractory	#	674	99	75	489	0	11	0
		%	100.00%	14.69%	11.13%	72.55%	0.00%	1.63%	0.00%
	Reactive	#	1832	260	119	1304	4	123	17
		%	99.73%	14.19%	6.50%	71.18%	0.22%	6.71%	0.93%
	Product	#	18	2	7	6	0	1	0
		%	88.89%	11.11%	38.89%	33.33%	0.00%	5.56%	0.00%
P2 Bacteria+light	Refractory	#	1223	136	120	963	4	0	0
		%	100.00%	11.12%	9.81%	78.74%	0.33%	0.00%	0.00%
	Reactive	#	715	69	22	554	0	48	20
		%	99.72%	9.65%	3.08%	77.48%	0.00%	6.71%	2.80%
	Product	#	693	75	38	517	1	24	37
		%	99.86%	10.82%	5.48%	74.60%	0.14%	3.46%	5.34%

Appendix D. Comparison of DOM compounds from FW streams and PW streams prior to and after products prior to and after bacteria-only, light-only, and bacteria+light incubations by index analysis

ID	Time Point		Total	Sum Identified	CARS DBE/C >0.7	Modified AI 0.5 ~ 0.67	Modified AI >0.67	Aliphatic	CRAM	Black carbon-like components
F1 Bacteria-only	T_0	#	3083	1941	199	767	146	382	1167	353
		%	100.00%	62.96%	6.45%	20.14%	4.74%	12.39%	37.85%	6.25%
	T_{15}	#	3063	1905	193	616	140	349	1179	349
		%	100.00%	62.19%	6.30%	20.11%	4.57%	11.39%	38.49%	5.95%
F2 Bacteria-only	T_0	#	2576	1643	231	686	149	246	1090	392
		%	100.00%	63.78%	8.97%	20.85%	5.78%	9.55%	42.31%	8.12%
	T_{15}	#	2576	1666	198	463	122	235	1198	331
		%	100.00%	64.67%	7.69%	17.97%	4.74%	9.12%	46.51%	5.39%
P1 Bacteria-only	T_0	#	2506	1589	26	291	15	622	846	68
		%	100.00%	63.41%	1.04%	11.01%	0.60%	24.82%	33.76%	0.87%
	T_{15}	#	1386	1108	2	36	6	348	729	18
		%	100.00%	79.94%	0.14%	2.60%	0.43%	25.11%	52.60%	0.42%
P2 Bacteria-only	T_0	#	1938	1441	16	146	6	608	816	43
		%	100.00%	74.36%	0.83%	7.53%	0.31%	31.37%	42.11%	0.72%
	T_{15}	#	2449	1731	101	339	43	518	1133	201
		%	100.00%	70.68%	4.12%	13.84%	1.76%	21.15%	46.26%	3.13%
F1 Light-only	T_0	#	2899	1767	225	594	179	411	916	368
		%	100.00%	60.95%	7.76%	20.49%	6.17%	14.18%	31.60%	7.14%
	T_{15}	#	1983	1434	22	81	22	252	1148	30
		%	100.00%	72.31%	1.11%	4.08%	1.11%	12.71%	57.89%	0.37%

P1 Bacteria+light	T_0	#	2506	1589	26	291	15	622	846	68
		%	100.00%	63.41%	1.04%	11.01%	0.60%	24.82%	33.76%	0.87%
	T_{15}	#	692	518	0	5	0	204	313	0
		%	100.00%	74.86%	0.00%	0.72%	0.00%	29.48%	45.23%	0.00%
P2 Bacteria+light	T_0	#	1938	1441	16	146	6	608	816	43
		%	100.00%	74.36%	0.83%	7.53%	0.31%	31.37%	42.11%	0.72%
	T_{15}	#	1916	1494	0	36	0	469	1025	1
		%	100.00%	77.97%	0.00%	1.88%	0.00%	24.48%	53.50%	0.01%